# Strategy for the Management of Thermodynamic Data with Application to Practical Cases of Systems Formed by Esters and Alkanes through Experimental Information, Checking-Modeling, and Simulation

Raúl Rios, Juan Ortega,* Adriel Sosa, and Luis Fernández

Laboratorio de Termodinámica y Fisicoquímica de Fluidos (ITI-IDeTIC), Parque Científico-Tecnológico, Universidad de Las Palmas de Gran Canaria, 35071 Canary Islands, Spain

S *Supporting Information*

ABSTRACT: In this work, a methodology is established to manage and use, in a more rigorous way, the experimental information that reflects the thermodynamic—mathematical behavior of dissolutions. The management of experimental information is carried out with an application on binaries of esters and alkanes which is useful in any other case. Specifically, for this work a new real database (of several properties under different conditions) is generated for eight binaries formed by four alkanoates, with a carbon number number ≥ 4, and two alkanes C_6 and C_8. A sequence of operations is proposed, ranging from experimentation to simulation, with two highly relevant intermediate stages, modeling↔ verification of the quality of data, whose impact on the simulation is evaluated. The experimental contribution of some properties v^E, c_P^E, h^E, g^E, gives rise to two very important operations, such as the combined modeling of the properties, taking into account the thermodynamic formalism, and the verification of the vapor—liquid equilibrium (VLE) data. For the latter process, the methodology designed in a previous work (*J. Chem. Thermodyn.* **2017**, *105*, 385) is put into practice, as well as a new method, rigorous under a thermodynamic—mathematical point of view, in which the modeling of properties is considered. The binomial *model-consistency test* is generated as a strategic stage to define the quality of the data. To achieve an accurate modeling in the multifunctional correlation that is proposed, two procedures are adopted: (a), step-by-step (SSO), according to the inverse order of the derivation of the Gibbs function, and another (b), by multiobjective optimization (MOO). The parametrization obtained by the latter is implemented in the commercial software of Aspen-Plus to design a rectification operation to purify the compounds of one of the studied systems, comparing the results with those that the simulator emits with the information estimated by UNIFAC.
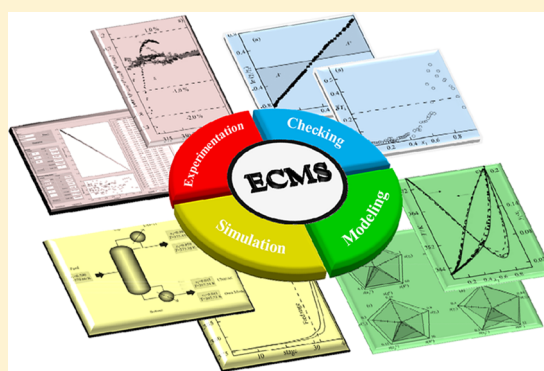
1. INTRODUCTION

The design of some operations in chemical engineering, such as extraction, distillation, absorption, etc., is based on the knowledge acquired from the phase equilibria, as pure compounds as solutions, depending on the case in question. Distillation is the operation studied the most, so it is essential to have accurate vapor—liquid equilibria data (VLE). At present, the theories do not accurately reproduce some of the complex scenarios that take place in these studies, such as the presence of azeotropes, the participation of nonvolatile components, etc. In any case, laboratory work is essential, but who or what can guarantee the quality of the experimentation, especially taking into account that the ultimate aim is to use these data to design real systems so that the chemical engineer can reach a predesigned engineering goal, the simulation. However, experimental information is not sufficient to characterize the behavior of solutions, requiring an adequate modeling. This work can, therefore, be considered as a way forward that goal as it combines several tools to ensure the transition from experimentation to design, providing experimental

and theoretical information for each of the blocks shown in Figure 1.

According to this scheme a methodology is proposed to manage the information of real data obtained for this work. The quality of data is analyzed to be used in the simulation of processes. Our research team has long-standing experience in experimentation on the properties of solutions, especially on those formed by esters and saturated hydrocarbons.[1−4] However, owing to a lack of data in the literature for isobaric vapor—liquid equilibria (iso-p VLE) of ester solutions with a high molecular weight, the **experimentation** conducted in this work provides VLE measurements at $p = 101.32$ kPa for eight binaries empirically formulated as: $C_{u−1}H_{2u−1}CO_2C_vH_{2v+1}$ ($u = 3, 4; v = 1, 2$) + C_nH_{2n+2} ($n = 6, 8$). Values for volumes v^E, enthalpies h^E, and thermal
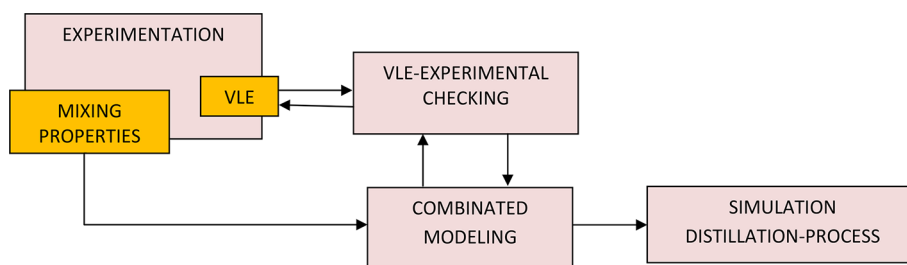
Figure 1. Scheme indicating the different thermodynamic—mathematical operations to validate the experimental information and its impact on the simulation of distillation processes

capacities c_P^E are presented at the same pressure but at several temperatures and are used to interpret the behavior of these solutions. More specifically, the experimentation carried out: v^E in the interval $T = [288.15-328.15]$ K, every 10 K, h^E at $T = [298.15, 318.15]$ K, and $c_P^E(T)$ over the range $T = [313.15-348.15]$ K. Previous data found in literature for the systems selected are: VLE,[6,7] azeotropes,[7,8] h^E,[9-15] v^E,[13-19] and γ_i^∞.[20,21] As well as increasing our knowledge of these solutions, the great quantity of measurements made can help us to progress toward other goals set in this work. Clearly, a huge amount of experimental information is needed, but of quality, since without this requirement, the following steps: **modeling** and **simulation** will not have enough rigor. In this work, therefore, a tool that accurately models the different properties of a multicomponent system is valued.

Modeling of the experimental values presented here is done by a multiparametric model that was used previously for different cases,[3,22,23] employing two parametrization procedures, multi-objective optimization[4,22,23] (MOO) with simultaneous correlation of all quantities, and another one, referred to as *sequential*, in which the properties are correlated by a step-by-step optimization (SSO) procedure[24] in reverse direction to the successive derivation of the Gibbs function, in other words: $c_P^E \rightarrow h^E \rightarrow g^E$. The well-known equation NRTL[25] is used to validate the capacity of the correlative model used for data treatment. Another goal of this work, in relation to the quality of the experimental information is to use a methodology, described in a previous work,[26] to analyze the quality of the iso-p VLE data presented. A rigorous method published recently by the authors[27] is applied with the new data for the first time. As a rule, testing of the **experimentation** is essential to guarantee the **modeling** operation and vice versa.

After carrying out the operations that have been highlighted before, it is practical to analyze the repercussion of two of them (**experimentation↔modelization**) in the **simulation** of a separation process, at least for one of the solutions whose values are presented here. It is solved with a method based on equilibrium stages, applied to one of the binaries, using the Aspen-Plus simulator.[28] In our case, it is necessary to implement in said software the proposed model in this work. In this way, a comparison of the simulation operation is made between the results obtained with the methodology described in Figure 1 and that by Aspen-Plus, checking the goodness of representation of both procedures, and especially analyzing the impact of the quality of the real data in the design operation of a rectification column.

2. EXPERIMENTAL SECTION

2.1. Materials. The compounds used, with the highest grade of commercial purity, were from Aldrich. Before experimentation they were degasified with ultrasound and stored in the dark over a 0.4 nm molecular sieves by SAFC. The water contents of the compounds were determined using a C20-Mettler Karl Fischer

titrator and in all cases were lower than 135 ppm. After these treatments, the final purity of the substances, measured by GC (Varian-450), was found to be higher than those provided by the manufacturer. Moreover, the quality of the compounds was tested by measuring several properties such as the normal boiling point $T_{b,i}^o$/K, density ρ/kg·m^{-3}, refractive index n_D, and thermal capacity c_p/J·mol^{-1}·K^{-1} . These values are recorded in Table S1 (Supporting Information), and comparisons with values published in the literature[29-35] are acceptable.

2.2. Apparatus and Procedures. The measurements of properties of the pure compounds were made at several temperatures within the interval $[288.15-328.15]$ K. The n_D were measured by a Zuzi 320 Abbe-type refractometer with a reading error of $(n_D \pm 2 \times 10^{-4})$ and whose temperature at $(T \pm 0.01)$ K was controlled by a Hetobirkeroad-CB7 circulating water bath. The refractometer was calibrated with bidistilled and degassified water using the values of $n_D(T)$ from the literature.[29] Measurements of $\rho(T)$ were made with an Anton-Paar 60/602 digital densimeter with a reading error of $(\rho \pm 0.02)$ kg·m^{-3}. The cell temperature was maintained quasi-constant with the abovementioned circulating water bath, obtaining digitally the values in an Anton-Paar digital thermometer, model CKT-100. The densimeter was calibrated at each temperature with water and nonane.[30]

The c_p's were measured in a C80 calorimeter from Setaram, with a temperature control of $(T \pm 0.01)$ K and a resolution lower than 1%. Measurements were made by defining a thermogram in the range $(303.15-353.15)$ K and a ramp of 0.1 K; the upper limit for the hexane was established at 328.15 K, since T_b^o = 352.75 K (see Table S1). Values of c_p were calculated by the known three-stage procedure

$$c_p(T) = (\Delta F_{sample}/\Delta F_{reference})(m_{reference}/m_{sample})c_{p,reference}(T)$$

$$(1)$$

where ΔF correspond to the differences in area under the curve corresponding to the flow of energy exchanged between the sample and the reference substance (water) relative to the empty cell, obtained on the temperature ramp established at the working pressure. The procedure followed was verified with values obtained for heptane, which were reliable when compared with values from literature,[31] presenting an average percentage error lower than 1%. The values corresponding to the excess property of the binaries c_p^E, were calculated from the data obtained for the pure compounds and the synthetic mixtures prepared as explained later.

The excess volumes v^E were calculated from the density ρ of synthetic solutions of known composition. The pairs (x_1, ρ) were used to assess (x_1, v^E) at each temperature. The uncertainty of v^E was estimated to be $\pm 2 \cdot 10^{-9}$ m^3·mol^{-1}, while that of the composition was of $(x \pm 0.0003)$.

The mixing enthalpies, h^E, were measured directly in a Calvet-MS80D conduction calorimeter by Setaram, which operates quasi-isothermically with a temperature control of ± 1 mK. The apparatus was calibrated by a dynamic method, generating an analogous thermal process to that of the mixing process. Nonetheless, correct functioning of the apparatus was verified at the working temperatures (298.15 and 318.15) K obtaining measurements for the system propanol + benzene,[36] recording a mean error of less than 1%.
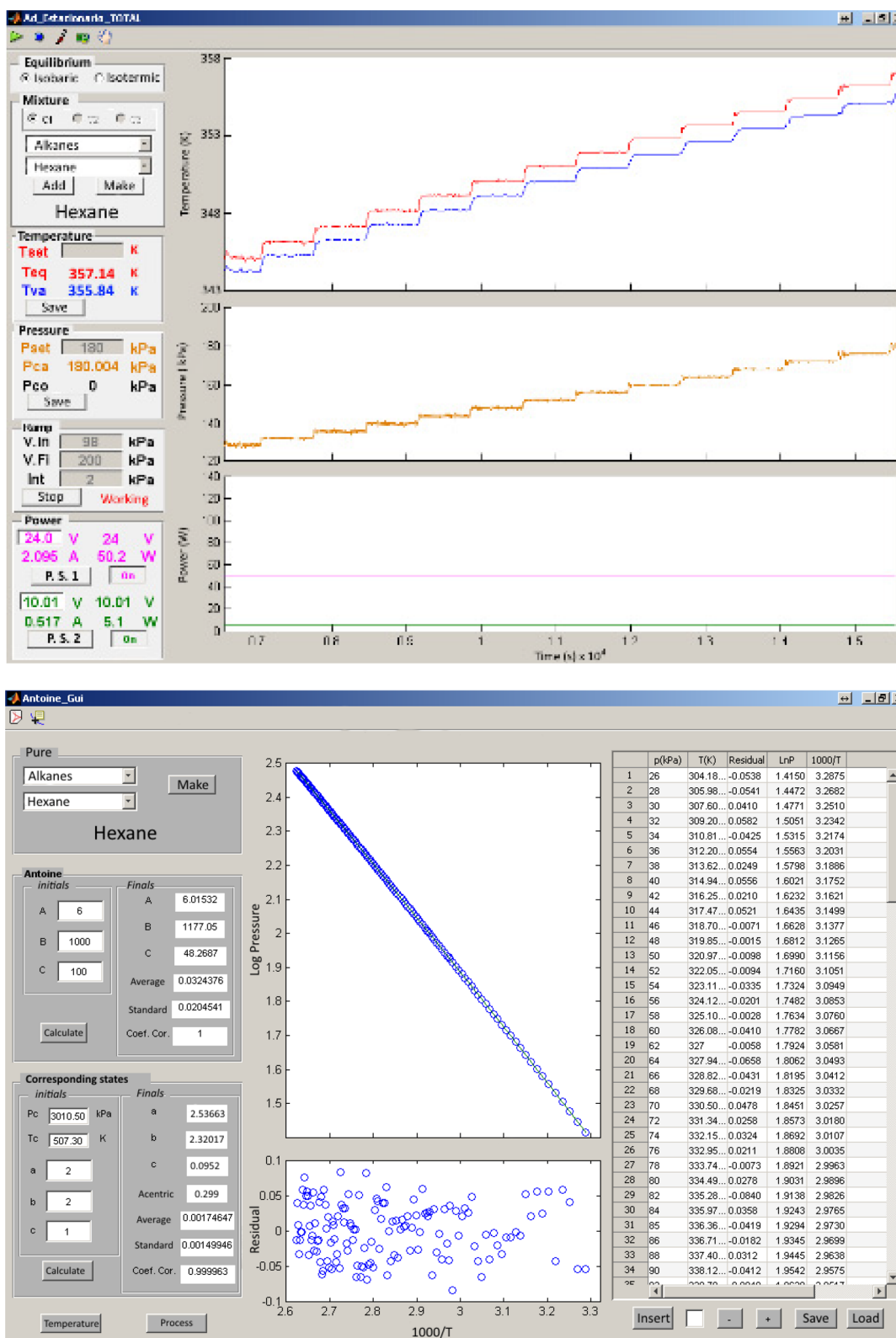

Figure 2. (a) Display of control variables as a function of time in the measurements of vapor pressures in a specified range. Pressure (yellow line), temperature (red line), and electric power (blue line). (b). Display of (T, p_i^o) values for hexane, showing the experimental points (◯) according to the Antoine equation, and the corresponding residuals.

Vapor pressures (T, p_i^o) and iso-p VLE data were obtained in an ebulliometer with recirculation of both phases, described in a previous study.[37] The pressure was controlled $(p \pm 0.02)$ kPa throughout the experiment using a DH-PPC2 instrument, and the temperature was measured by a Comark-6900 digital thermometer equipped with two Pt100 probes calibrated according to ITS-90, with a reading error of ± 20 mK. In a previous work,[5] a scheme of the installation was presented, which has been modified to improve the pressure regulation. Two power sources were used (Promax, FA-405) programmed with PC by RS232, which achieved real equilibrium states by establishing stable power values (0.1%), optimum for the two heating areas (boiler T_1, and main body T_2), fulfilling that: $\Delta T = (T_1 - T_2) < 1$ K. To obtain the (T, p_i^o) values the system worked automatically with inputs to PC establishing (partial and global) pressure intervals for each compound. Figure 2 shows the information displayed on two PC screens for data of (T, p_i^o) for the hexane, automatically operating over a previously fixed p interval, using a software coded in Matlab. This regulates the automatic functioning of the auxiliary variables (pressure, temperature and electrical power), establishing a standard working procedure for data recording. The experiment starts with the lowest value of p; the output given by the PC to the DH-PPC2 establishes the working temperature of the ebulliometer. This was maintained constant for ~17 min, the estimated time to guarantee an equilibrium state for both phases. This condition is achieved when the variables (p, T) remain constant. The operation is repeated by increasing the set-point of the PPC2 by 2 kPa and fine-tuning the power provided by the power sources. Repeatedly, a step scanning carried out until the desired maximum pressure of approximately 300 kPa is achieved.

To determine the iso-p VLE, the working pressure was maintained constant at (101.32 ± 0.02) kPa and for the mixtures a similar approach was followed to the one described above, although a more detailed description can be found in a previous work.[5] With slight changes to the software used (in relation to temporality), the variables that define the iso-p VLE states were defined. Samples of the phase equilibria were analyzed by densimetry, and uncertainties for the liquid phases compositions were estimated to be around $(x \pm 0.002)$, and around $(y \pm 0.003)$ for the vapor phase.

3. PRESENTATION OF RESULTS AND MODELING

3.1. Properties of Pure Compounds. Densities ρ of pure compounds were measured every 10 K in the interval $[288.15-328.15]$ K, and the values are shown in Table S2. These were used to calculate the expansion coefficients, $\alpha = -(d \ln \rho/dT)$, compiled in Table S1. The mean values of α_i (over the interval of temperatures measured) are used to evaluate the saturation volumes of pure compounds such as is indicated later.

The c_p's of pure compounds were determined at several temperatures, and the values obtained are shown in Table S3. The functional $c_p = c_p(T)$ is linear and its coefficients, obtained by least-squares regression, are recorded in Table S4. Figure 3 shows the variation in c_p with temperature for the compounds studied here and a comparison of the data with values from literature.[31] The greatest differences, ~2%, can be observed in the inset-graph for ethyl propanoate, as the values for this compound appear to be interchanged with values found for methyl butanoate, determined in 1898 by Schiff et al. (see ref 31). The concordance of the remaining data with those from literature is acceptable over the entire temperature range selected. For hexane and methyl propanoate a limited temperature range was used; see Table S3.

The boiling points obtained in the ebulliometer are an indication of the purity of the compounds and are recorded in Table S1
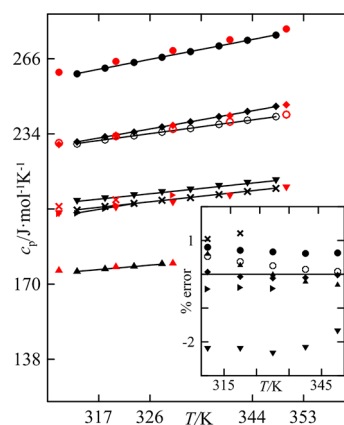
Figure 3. Thermal capacities of pure substances: (▲) methyl propanoate, (▼) ethyl propanoate, (×) methyl butanoate, (○) ethyl butanoate, (▶) hexane, (◆) heptane, (●) octane. The corresponding red symbols are extracted from the literature.[31] Inset figure: % error = $100 \left(c_p^{exp} - c_p^{lit}\right)/c_p^{exp}$.

and compare well with those in the literature. New values were determined for the vapor pressures p_i^o of pure compounds with the purpose of increasing the useful interval that can be used to correlate the data pairs (T, p_i^o) obtained experimentally. Repercussion of the data, or their correlations $p_i^o = \varphi(T)$, on the characterization of equilibrium phases is important. Hence, periodically, new measurements (T, p_i^o) are made in our laboratory to obtain more accurate data, either by changing the measuring intervals or by modifications in the apparatus and control installations as was done for this work, section 2.2. Therefore, having a greater automation in order to avoid the external manipulation, new (T, p_i^o) measurements were made. The values recorded for the esters were almost identical to those published previously,[3,5] and it was deemed unnecessary to present here the new values. However, this was not the case for the two hydrocarbons, since the new measurements differed significantly from the published values.[1] Table 1 shows the values obtained with the automatic system described, every 2 kPa as indicated in section 2.2. Figure 4a shows the differences between the new experimental values and those from literature.[1,38-42] It can be observed that the greatest differences correspond with data published by Sauermann,[38] for hexane higher than 1% in the interval $T < 380$ K.

Values in Table 1 were correlated with Antoine's equation using an adequate algorithm; parameters A, B, and C are presented in Table 2. The reduced form of the Antoine equation establishes an approximation for the acentric factor ω by the expression $(\omega + a + 1)(0.7 - c) = b$, obtained using the definition of Pitzer,[43] where a, b, and c, are the parameters corresponding to the mentioned equation in reduced coordinates,[44] for which the values for the hydrocarbons are shown in Table 2. The ω obtained here present slight differences with those recorded in the literature[1,40] and with those estimated by the method of Lee-Kesler.[45] Although these coefficients can be calculated by establishing boundary conditions at the critical point, which are not always fulfilled owing to the limitations of Antoine's equation here these parameters were obtained by means of a direct correlation of the equation in reduced coordinates. Figure 4b shows the vapor pressures-lines for the pure components using the corresponding equation in reduced coordinates.

3.2. Properties of Binary Solutions and Data Treatment. The properties generated in the mixing processes were determined for eight binaries: $CH_3(CH_2)_{u-2}COO\ C_vH_{2v+1}(u = 3, 4; v = 1, 2)$ (1) + C_nH_{2n+2} $(n = 6, 8)$ (2) at several temperatures.

Table 1. Experimental Vapor Pressures for Alkanes

T (K)	p_i^o (kPa)	T (K)	p_i^o (kPa)	T (K)	p_i^o (kPa)	T (K)	p_i^o (kPa)	T (K)	p_i^o (kPa)	T (K)	p_i^o (kPa)
					hexane						
304.18	26.00	332.15	74.00	346.76	118.00	358.42	166.00	367.69	214.00	375.49	262.00
305.98	28.00	332.95	76.00	347.30	120.00	358.85	168.00	368.05	216.00	375.80	264.00
307.60	30.00	333.74	78.00	347.85	122.00	359.24	170.00	368.40	218.00	376.10	266.00
309.20	32.00	334.49	80.00	348.39	124.00	359.68	172.00	368.74	220.00	376.39	268.00
310.81	34.00	335.28	82.00	348.92	126.00	360.10	174.00	369.08	222.00	376.69	270.00
312.20	36.00	335.97	84.00	349.45	128.00	360.51	176.00	369.42	224.00	376.99	272.00
313.62	38.00	336.36	85.00	349.98	130.00	360.92	178.00	369.77	226.00	377.27	274.00
314.94	40.00	336.71	86.00	350.48	132.00	361.30	180.00	370.10	228.00	377.56	276.00
316.25	42.00	337.40	88.00	351.00	134.00	361.72	182.00	370.44	230.00	377.85	278.00
317.47	44.00	338.12	90.00	351.49	136.00	362.12	184.00	370.76	232.00	378.42	282.00
318.70	46.00	338.79	92.00	352.00	138.00	362.50	186.00	371.10	234.00	378.71	284.00
319.85	48.00	339.47	94.00	352.48	140.00	362.89	188.00	371.42	236.00	378.99	286.00
320.97	50.00	340.11	96.00	352.98	142.00	363.28	190.00	371.74	238.00	379.28	288.00
322.05	52.00	340.79	98.00	353.43	144.00	363.66	192.00	372.06	240.00	379.56	290.00
323.11	54.00	341.40	100.00	353.91	146.00	364.04	194.00	372.40	242.00	379.84	292.00
324.12	56.00	341.82	101.33	354.38	148.00	364.41	196.00	372.72	244.00	380.12	294.00
325.10	58.00	342.03	102.00	354.85	150.00	364.80	198.00	373.02	246.00	380.39	296.00
326.08	60.00	342.65	104.00	355.32	152.00	365.17	200.00	373.35	248.00	380.66	298.00
327.00	62.00	343.25	106.00	355.76	154.00	365.53	202.00	373.65	250.00	380.94	300.00
327.94	64.00	343.87	108.00	356.21	156.00	365.90	204.00	373.97	252.00		
328.82	66.00	344.47	110.00	356.66	158.00	366.26	206.00	374.28	254.00		
329.68	68.00	345.04	112.00	357.12	160.00	366.62	208.00	374.59	256.00		
330.50	70.00	345.61	114.00	357.55	162.00	366.97	210.00	374.89	258.00		
331.34	72.00	346.19	116.00	357.99	164.00	367.35	212.00	375.20	260.00		
					octane						
343.50	16.00	384.08	66.00	402.43	112.00	416.59	162.00	427.65	212.00	436.87	262.00
346.28	18.00	385.08	68.00	403.09	114.00	417.09	164.00	428.07	214.00	437.23	264.00
349.04	20.00	386.00	70.00	403.72	116.00	417.56	166.00	428.46	216.00	437.53	266.00
351.55	22.00	386.96	72.00	404.36	118.00	418.03	168.00	428.85	218.00	437.89	268.00
353.90	24.00	387.89	74.00	404.99	120.00	418.53	170.00	429.24	220.00	438.20	270.00
356.09	26.00	388.77	76.00	405.63	122.00	418.97	172.00	429.64	222.00	438.55	272.00
358.12	28.00	389.67	78.00	406.23	124.00	419.47	174.00	430.02	224.00	438.88	274.00
360.05	30.00	390.48	80.00	406.85	126.00	419.91	176.00	430.38	226.00	438.88	274.00
361.89	32.00	391.36	82.00	407.43	128.00	420.38	178.00	430.76	228.00	439.22	276.00
363.62	34.00	392.15	84.00	408.04	130.00	420.84	180.00	431.15	230.00	439.53	278.00
365.27	36.00	392.98	86.00	408.61	132.00	421.27	182.00	431.53	232.00	439.86	280.00
366.87	38.00	393.81	88.00	409.17	134.00	421.72	184.00	431.88	234.00	440.19	282.00
368.39	40.00	394.59	90.00	409.72	136.00	422.18	186.00	432.26	236.00	440.52	284.00
369.88	42.00	395.37	92.00	410.28	138.00	422.61	188.00	432.63	238.00	440.82	286.00
371.26	44.00	396.14	94.00	410.86	140.00	423.04	190.00	432.98	240.00	441.14	288.00
372.61	46.00	396.87	96.00	411.40	142.00	423.48	192.00	433.34	242.00	441.46	290.00
373.94	48.00	397.62	98.00	411.96	144.00	423.93	194.00	433.71	244.00	441.77	292.00
375.19	50.00	398.34	100.00	412.50	146.00	424.33	196.00	434.08	246.00	442.08	294.00
376.40	52.00	398.70	101.00	413.03	148.00	424.76	198.00	434.42	248.00	442.38	296.00
377.61	54.00	398.82	101.33	413.54	150.00	425.21	200.00	434.80	250.00	442.69	298.00
378.74	56.00	399.02	102.00	414.08	152.00	425.62	202.00	435.14	252.00	443.01	300.00
379.87	58.00	399.76	104.00	414.56	154.00	426.04	204.00	435.49	254.00		
380.92	60.00	400.41	106.00	415.10	156.00	426.43	206.00	435.85	256.00		
382.04	62.00	401.10	108.00	415.57	158.00	426.85	208.00	436.18	258.00		
383.07	64.00	401.75	110.00	416.09	160.00	427.27	210.00	436.54	260.00		

Table S2 shows the experimental data of (x_1, ρ, v^E) at five temperatures in the interval $[288{-}328]$ K. Although the literature contains v^E data at 298.15 K, new measurements of (x_1, ρ) were made to confirm these values and for use in the modeling process. A comparison of the v^E with those recorded in the literature[15−17] in Figure S1(a) ,(b) show slight differences between the data series.

The information obtained for all the excess properties (v^E, h^E, c_p^E) was correlated using a polynomial expression in the *active fraction* z_i, represented generically by $y^E = \varphi[z_i(x_i)]$

$$y^E(x, T) = z_1 z_2 \sum_{i=0}^{2} y_i z_1^i$$

(2)

where:

$$y_i = \sum_{j=0}^{2} Y_{ij} T^{j-1} = \frac{Y_{i0}}{T} + Y_{i1} + Y_{i2} T; \quad z_1 = x_1/(x_1 + k_Y x_2)$$

(3)

with k_Y being a particular parameter and whose meaning will be discussed later. The functional eq 2 is used to correlate the
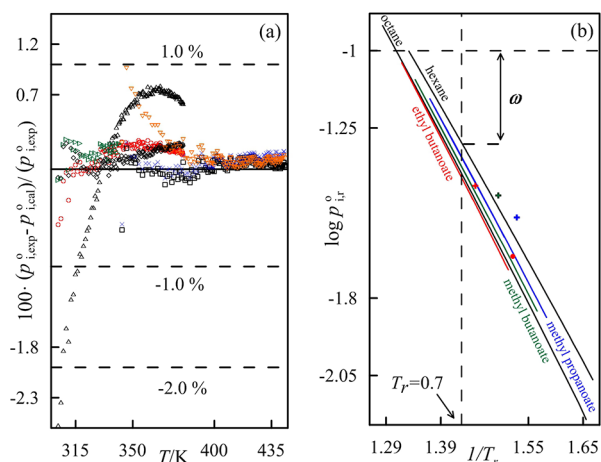
Figure 4. (a) Comparison of experimental p_i^o data with those from literature: hexane: ($\triangle$) ref 1, ($\diamond$) ref 32, ($\triangleright$) ref 33, ($\bigcirc$) ref 35; octane: ($\triangledown$) ref 1, ($\times$) ref 34, ($\square$) ref 36. (b) Vapor pressures lines in reduced coordinates for the compounds of this work and azeotropic points for methyl propanoate (1) + hexane (2) (blue +), ethyl butanoate (1) + octane (2) (red +) and methyl butanoate (1) + octane (2) (green +). Azeotrope (●) at 60 kPa (ref 7) for ethyl butanoate (1) + octane (2).

properties arising from the mixing processes, and in all cases the same correlation procedure described here is followed. Values of $y^E = y^E(x_1,T)$ are correlated individually for each binary using a nonlinear regression method, based on least-squares and programmed in Matlab with the following objective function, OF

$$\text{OF} = s(y^E) = \left[\sum_{i=1}^{N} (y_{i,\text{exp}} - y_{i,\text{cal}})^2 / (N-1) \right]^{1/2} \tag{4}$$

with minimization of the OF, the coefficients Y_{ij} of eq 3 are obtained for each property v^E, h^E and c_p^E, which we call V_{ij}, H_{ij}, and C_{ij}, respectively. Results are shown in Table S7. The valuation of all the fits is good.

The coefficient k_Y of eq 3 merits a special mention in the data treatment. This parameter (dependent on p and T) depends on the solution and the property represented, however, here we consider it pressure-independent due to the practical incompressibility of the liquid phase. Hence, for correlation of volumes this parameter is considered to be the quotient of the molar volumes of the pure compounds ($k_v \equiv k_Y$) in the solution and for the binary is: $k_v = [\nu_2^o(p,T)/\nu_1^o(p,T)]$. If we now consider the renowned equation of state in relation to the coefficients α and β

$$\frac{dv}{v} = \frac{1}{v}\left(\frac{\partial v}{\partial T}\right)_P dT + \frac{1}{v}\left(\frac{\partial v}{\partial p}\right)_T dp = \alpha dT - \beta dp \tag{5}$$

whose integration, taking average values for α and β in the experimental range of temperatures and pressures ($dp = 0$), generates the following expression for k_v.

$$k_v(T) = \frac{\nu_2^o}{\nu_1^o} = \frac{\nu_{2,\text{ref}}^o \exp[\alpha_2(T - T_{\text{ref}})]}{\nu_{1,\text{ref}}^o \exp[\alpha_1(T - T_{\text{ref}})]} = k_{v,0}$$
$$\exp[(\alpha_2 - \alpha_1)(T - T_{\text{ref}})] \tag{6}$$

This expression justifies the calculation of coefficients α_I exposed in Table S1. Now, $k_{v,0} = \nu_2^o(T_{\text{ref}})/\nu_1^o(T_{\text{ref}})$ is the quotient of molar volumes of the compounds involved in the binary, at the reference temperature T_{ref}=298.15 K; values of $k_{v,0}$ are recorded in Table S7. The combined modeling performed provides a good representation of the volumetric behavior of the solutions, with an acceptable representation of $v^E = v^E(x,T)$.

Table S5 shows the experimental data for (x_1, h^E) at 298.15 and 318.15 K for the systems studied. Although data were published previously for the methyl ester solutions,[14,15] the new measurements were similar to those. However, the new h^E data formed by ethyl propanoate with the two hydrocarbons presented certain incoherences with those published.[13] In this case, $h^E = h^E(x,T)$ were correlated with eqs 2 and 3 but making $Y_{i2} = 0$ to avoid problems of *overfitting*, as data were only available at two temperatures. With regard to parameter k_Y of eq 3, this takes a different significance to the previous one and is called $k_h \equiv k_Y$, generating the following expression

$$k_h(T) = \frac{q_2}{q_1}\left[\frac{r_1}{r_2}k_v(T)\right]^{2/3}$$
$$= \frac{q_2}{q_1}\left[\frac{r_1}{r_2}k_{v,0} \exp[(\alpha_2 - \alpha_1)(T - T_{\text{ref}})]\right]^{2/3} \tag{7}$$

where r_k and q_k are, respectively, the Van der Waals volume and surface parameters for each molecule calculated by Bondi's group contribution method.[46] The coefficients obtained in the previous correlation process are recorded in Table S7 and produced acceptable values of $s(h^E)$. The enthalpic values and the fitting curves are shown in Figure S1(c), where the values are quite similar to those published by Navarro et al.[9] and Lopez et al.,[10] as occurs with those published by Ortega et al.[13] for the binary ethyl propanoate + hexane. However, the same does not occur with data

Table 2. Coefficients A, B, and C of the Antoine Equation, $\log(p_i^o/\text{kPa}) = A - B/[(T/K) - C]$, Standard Deviation $s(p_i^o)$, Acentric Factors ω, and Temperature Range for Alkanes Used in This Work with Those from the Literature, $\log(p_{i,r}^o) = a - b/(T_r - c)$

compd	A	B	C	$s(p_i^o)$	ω	range T (K)	ref
hexane	6.01532	1177.05	48.27	0.032		304−381	this work
	(2.5366)	(2.3202)	(0.0952)		0.299		
					0.298^b		
	5.97830	1154.37	51.29		0.294	293−364	1
	6.00266	1171.53	48.78			286−342	38^a
					0.300		44
octane	6.05247	1356.84	63.52	0.043		343−443	this work
	(2.6563)	(2.3858)	(0.1117)		0.399		
					0.400^b		
	6.00660	1324.70	67.72		0.393	351−425	1
	6.04867	1355.13	63.63			326−399	38^a
					0.399		44

^{a}Recommended by NIST, ^{b}Estimated by the Lee-Kesler method.[45]

of the binary with octane, which are lower (around 150 Jmol^{-1}) than those from the same publications above.

The c_p^E's of the binaries are calculated by:

$$c_p^E = c_p - (x_1 c_{p,1} + x_2 c_{p,2}) \tag{8}$$

The numerical values of c_p^E are recorded in Table S6, while Figure S2 reflects the situation of the discrete values and 3D-surfaces constructed with a functional of the type $c_p^E = c_p^E(x_1,T)$, obtained by correlating the data with eqs 2 and 3 making (as in the correlation of h^E) $Y_{i2} = 0$. In this case, the parameter k_Y of eq 3 is called k_C and is determined as an additional parameter using the same optimization procedure mentioned previously. The results of the correlation are shown in Table S7, and Figure S2 shows some scattering of the surfaces $c_p^E = c_p^E(x_1,T)$ and the experimental points, as shown in Figure S3 for one of the systems. After describing the procedures used to represent mathematically data for the eight binaries elected and the graphs generated, the behavior of the solutions is discussed now. On the whole, the surfaces of $c_p^E = c_p^E(x_1,T)$ appear to give a good representation of a ω-shape behavior, mentioned in previous works for this type of systems.[4,47] This effect should become relevant in the functional $h^E = h^E(T)$ but is negligible for the systems studied; in other words, the gradients $(\partial h^E/\partial T)_p$ are small in spite of the high values of h^E due to the endothermic effect of the mixing processes. This behavior of esters in solutions with alkanes is due to the variation of their polarity with temperature which affect to the thermal capacities. Additionally, there is a conformational equilibrium (*s-cis* and *s-trans*) that is affected by any change; i.e., the presence of alkanes changes the dipole moments displacing the aforementioned equilibrium. This is also reflected in the expansions of the final solutions that are formed, with $v^E > 0$ and with $(\partial v^E/\partial T)_p > 0$. The two thermal coefficients decrease with increasing molecular weight of the ester since the rise in temperature has little repercussion on the mixing properties. This is as expected, since the relative expansion in the case of large molecules, such as the alkanoates studied here, is less pronounced. To summarize, the net effects produced in the mixing processes are noteworthy, clearly reflecting two factors. On the one hand, the increase in the ester chain (from propanoate to butanoate, for example, or from methyl to ethyl, which favors the presence of centers of apolar interaction). On the other hand, the resulting increase in the permanent dipolar moment μ, should produce an increase in dipole−dipole attractions, both of the pure compounds and of the final mixture, although less extreme in the latter due to the greater intermolecular distance. The dipole−dipole interactions increase as the size of the ester diminishes, the opposite process results in a better apolar association of the hydrocarbons, reducing the dipole−dipole effect in the pure ester. However, in spite of these observations, the experimental results show that the dipolar effect is much less significant than the effect that dominates in these systems, which is the size of the ester molecule.

3.3. Vapor−Liquid Equilibria. Experimental values of iso-101.32 kPa VLE (T,x_1,y_1) for the eight binaries already mentioned are shown in Table 3, and the points corresponding to the variables are graphically represented as T vs x_1,y_1 and $(y_1 - x_1)$ vs x_1 in Figure 5. The activity coefficients for each species in the different equilibrium stages are calculated by the *gamma-phi* approach, expressed as

$$\ln \gamma_i = \ln\left(\frac{y_i p}{x_i p_i^o}\right) + \ln\left(\frac{\hat{\phi}_i}{\phi_i^o}\right) + \frac{v_i^o(p_i^o - p)}{RT} = \ln\left(\frac{y_i p}{x_i p_i^o}\right) + \ln \Phi_i \tag{9}$$

or $\Phi_i = (\hat{\phi}_i/\phi_i^o) + factor\ de\ Poynting$, where the first summand is the quotient between the fugacity coefficients of compound i in the solution and of the pure product, which are calculated in a simple way from the truncated virial equation. Equation 9 can be rewritten as

$$\ln \gamma_i = \ln\left(\frac{p y_i}{x_i p_i^o}\right) + \frac{(B_{ii} - v_i^s)(p - p_i^o)}{RT} + \frac{p}{RT}(2B_{ij} - B_{ii} - B_{jj})y_j^2 \tag{10}$$

where p_i^o is the vapor pressure of compound i, calculated using Antoine's equation as was indicated above. The second virial coefficients B_{ii} are calculated from the expressions by Tsonopoulos[48] and those of the mixtures of B_{ij} using one of the classic combination methods.[49] For molar volumes at saturation v_i^s, an equation similar to that of the numerator (or denominator) of eq 6 was used, which was obtained with experimental information in this work. The γ_i of eq 10 are used to calculate the adimensional Gibbs function values: $g^E/RT = \Sigma x_i \ln \gamma_i$, of each stage recorded in Table 3. Before continuing with the tasks outlined in Figure 1, **modeling→simulation**, the quality of VLE data must be verified thermodynamically. The calculated thermodynamic quantities characteristic of VLE's are reflected in Figure 6, and this is used here for the analysis of checking the quality of data.

3.3.1. Thermodynamic Consistency of VLE Data. As mentioned, the quality of the experimental VLE data directly influences on the design of the separation process. Recently,[26] some recommendations were made to analyze the thermodynamic consistency of VLE data using some of the methods known in the field of equilibrium thermodynamic. Due to the interest that this subject raises, here puts into practice the verification methodology recommended, specifying the details of the different steps of the procedure. One step required prior to applying consistency methods is that of data reduction based on graphical visualization of the results, (a). Later, several known tests are applied: (b) the area test[50] and (c) those of Fredenslund,[51] (d) Wisniak,[52] (e) Kojima,[53] and (f) Van Ness.[54] The Supporting Information (Figure S4) shows the graphs obtained by the different methods applied to the binaries which, as can be observed in Table 4, present extreme valuations. Finally, a new section introduces the application of a new test proposed by the authors for binaries,[27,55] which we consider to be rigorous.

Application of the first methods (a)−(f), gives rise to the following comments:

(a) *Graphical reduction of the data obtained* (directly or indirectly) using the representations $T = T(x_1,y_1)$ and $\gamma_i = \gamma_i(x_1,y_1)$, is the first step to verify their quality. On observation of the values, an initial crude elimination of some data can first be done, followed by a fine-tuning of the graphs obtained, finally resulting in Figures 5 and 6. In Figures 5e and 6e, at $x_1 \approx 0.25$ one point is observed for the system methyl propanoate (1) + octane (2) that lies outside the trend followed by the rest. However, this is an isolated case and appears to be associated with a random error in the experimentation. Some deficient values are also observed in the regions close to infinite dilution. For solutions of methyl propanoate and butanoate with octane, Figures 6e,g, present a maximum in the curve of γ_1, at $x_1 \approx 0.18$, which does not coincide with a minimum in the corresponding γ_2; this is a sign of inconsistency,

Table 3. Experimental and Calculated Properties for the Isobaric VLE of Binaries Alkyl Alkanoate (1) + an Alkane (2) at 101.32 kPa

T (K)	x_1	y_1	γ_1	γ_2	g^E/RT	T (K)	x_1	y_1	γ_1	γ	g^E/RT
					methyl propanoate (1) + hexane (2)						
341.82	0.000	0.000		1.000	0.000	339.54	0.386	0.350	1.403	1.134	0.208
341.57	0.012	0.019	2.312	1.001	0.010	339.59	0.400	0.358	1.381	1.145	0.210
341.44	0.018	0.029	2.279	1.001	0.016	339.69	0.433	0.375	1.329	1.177	0.216
341.32	0.025	0.038	2.216	1.002	0.022	339.87	0.463	0.393	1.293	1.202	0.218
341.18	0.032	0.049	2.207	1.002	0.028	340.06	0.496	0.410	1.254	1.235	0.219
341.03	0.042	0.061	2.155	1.004	0.035	340.15	0.511	0.419	1.239	1.251	0.219
340.87	0.052	0.075	2.115	1.005	0.044	340.29	0.528	0.429	1.220	1.270	0.218
340.59	0.072	0.099	2.036	1.009	0.059	340.48	0.549	0.444	1.209	1.285	0.217
340.37	0.090	0.119	2.001	1.011	0.072	340.71	0.576	0.460	1.182	1.320	0.214
340.18	0.108	0.139	1.950	1.014	0.085	340.92	0.598	0.474	1.166	1.347	0.211
340.01	0.126	0.158	1.903	1.018	0.097	341.26	0.628	0.493	1.142	1.387	0.205
339.87	0.144	0.176	1.866	1.021	0.108	341.45	0.643	0.503	1.129	1.411	0.201
339.73	0.165	0.194	1.805	1.029	0.121	341.65	0.658	0.513	1.117	1.436	0.197
339.65	0.183	0.210	1.768	1.033	0.130	341.92	0.677	0.528	1.109	1.459	0.192
339.56	0.202	0.225	1.721	1.040	0.141	342.26	0.700	0.545	1.094	1.498	0.184
339.51	0.219	0.239	1.684	1.046	0.150	342.78	0.726	0.572	1.087	1.523	0.175
339.46	0.228	0.247	1.677	1.048	0.154	343.55	0.759	0.606	1.073	1.556	0.160
339.45	0.233	0.249	1.656	1.053	0.157	344.28	0.793	0.638	1.056	1.629	0.144
339.45	0.235	0.251	1.652	1.053	0.158	345.17	0.822	0.674	1.044	1.662	0.126
339.46	0.237	0.252	1.646	1.054	0.158	346.48	0.863	0.728	1.028	1.740	0.100
339.42	0.248	0.259	1.623	1.059	0.164	346.78	0.874	0.742	1.025	1.778	0.094
339.40	0.264	0.271	1.592	1.067	0.170	348.06	0.906	0.796	1.016	1.818	0.071
339.38	0.279	0.282	1.565	1.074	0.177	348.46	0.917	0.812	1.011	1.870	0.063
339.39	0.297	0.293	1.532	1.083	0.183	348.97	0.928	0.833	1.009	1.892	0.054
339.40	0.313	0.304	1.508	1.090	0.188	349.95	0.949	0.875	1.003	1.965	0.037
339.41	0.327	0.313	1.483	1.099	0.193	350.46	0.959	0.896	1.001	1.989	0.029
339.43	0.342	0.322	1.462	1.108	0.197	350.90	0.968	0.916	1.000	2.011	0.022
339.46	0.358	0.332	1.439	1.117	0.201	351.22	0.975	0.933	1.000	2.055	0.018
339.50	0.372	0.341	1.419	1.126	0.204	352.75	1.000	1.000	1.000		0.000
					methyl propanoate (1) + octane (2)						
398.82	0.000	0.000		1.000	0.000	356.77	0.707	0.878	1.093	1.499	0.182
398.37	0.004	0.017	1.181	0.999	−0.001	356.35	0.732	0.887	1.079	1.552	0.173
397.79	0.009	0.035	1.226	1.000	0.002	356.15	0.746	0.891	1.071	1.582	0.168
397.18	0.013	0.051	1.216	1.003	0.006	355.97	0.758	0.895	1.065	1.613	0.163
396.49	0.017	0.073	1.313	1.003	0.008	355.79	0.770	0.899	1.059	1.638	0.157
394.72	0.030	0.122	1.327	1.009	0.017	355.60	0.783	0.903	1.052	1.675	0.151
393.48	0.038	0.156	1.348	1.012	0.023	355.43	0.794	0.908	1.048	1.689	0.145
388.80	0.072	0.277	1.428	1.022	0.046	355.27	0.806	0.912	1.042	1.737	0.140
385.74	0.096	0.351	1.457	1.028	0.061	355.09	0.819	0.916	1.036	1.775	0.133
379.78	0.150	0.482	1.486	1.040	0.093	354.94	0.831	0.921	1.031	1.804	0.126
377.30	0.176	0.529	1.489	1.050	0.110	354.76	0.844	0.925	1.026	1.857	0.118
374.78	0.204	0.574	1.482	1.063	0.129	354.60	0.856	0.930	1.022	1.893	0.111
369.56	0.278	0.670	1.465	1.072	0.156	354.45	0.868	0.935	1.018	1.930	0.103
368.46	0.307	0.687	1.402	1.096	0.167	354.29	0.881	0.940	1.013	1.983	0.093
366.27	0.349	0.721	1.375	1.119	0.184	354.12	0.893	0.945	1.010	2.041	0.085
364.82	0.383	0.746	1.353	1.127	0.190	353.99	0.904	0.950	1.007	2.092	0.076
363.65	0.417	0.765	1.317	1.146	0.194	353.85	0.915	0.954	1.004	2.158	0.068
362.33	0.460	0.785	1.273	1.182	0.201	353.67	0.929	0.961	1.001	2.209	0.058
361.15	0.502	0.804	1.237	1.218	0.205	353.45	0.947	0.970	0.998	2.312	0.043
360.10	0.543	0.820	1.202	1.264	0.207	353.38	0.952	0.973	0.998	2.343	0.038
359.38	0.570	0.831	1.186	1.294	0.208	353.20	0.966	0.980	0.996	2.438	0.027
358.86	0.595	0.840	1.167	1.323	0.205	353.12	0.978	0.986	0.993	2.553	0.014
358.44	0.616	0.847	1.151	1.352	0.203	353.01	0.988	0.993	0.992	2.620	0.004
358.01	0.639	0.855	1.135	1.386	0.199	352.98	0.992	0.995	0.992	2.680	−0.001
357.79	0.650	0.859	1.127	1.405	0.197	352.94	0.996	0.997	0.992	2.847	−0.004
357.59	0.664	0.863	1.116	1.425	0.192	352.75	1.000	1.000	1.000		0.000
357.24	0.683	0.870	1.105	1.456	0.187						
					ethyl propanoate (1) + hexane (2)						
341.82	0.000	0.000		1.000	0.000	347.76	0.434	0.248	1.236	1.118	0.155
342.00	0.014	0.010	1.945	0.999	0.008	348.03	0.455	0.256	1.208	1.140	0.158
342.05	0.020	0.014	1.952	0.999	0.012	348.81	0.487	0.277	1.189	1.151	0.156

Table 3. continued

T (K)	x_1	y_1	γ_1	γ_2	g^E/RT	T (K)	x_1	y_1	γ_1	γ	g^E/RT
					ethyl propanoate (1) + hexane (2)						
342.10	0.026	0.019	1.916	0.999	0.016	349.13	0.505	0.286	1.171	1.167	0.156
342.18	0.033	0.024	1.913	0.999	0.021	349.46	0.517	0.296	1.168	1.170	0.156
342.24	0.040	0.029	1.944	0.999	0.025	350.15	0.551	0.314	1.136	1.202	0.153
342.31	0.047	0.033	1.886	0.999	0.029	350.76	0.575	0.330	1.120	1.220	0.150
342.38	0.055	0.039	1.839	1.001	0.035	351.41	0.603	0.347	1.101	1.248	0.146
342.49	0.065	0.045	1.823	1.001	0.040	352.63	0.650	0.380	1.073	1.301	0.138
342.55	0.071	0.050	1.816	1.002	0.044	356.26	0.748	0.482	1.048	1.368	0.114
342.75	0.091	0.062	1.761	1.004	0.055	356.84	0.764	0.499	1.042	1.393	0.109
342.92	0.106	0.071	1.734	1.006	0.064	357.34	0.778	0.512	1.034	1.419	0.104
343.11	0.123	0.082	1.719	1.007	0.072	359.38	0.820	0.573	1.027	1.456	0.090
343.40	0.146	0.095	1.653	1.011	0.083	360.04	0.834	0.591	1.021	1.483	0.082
343.62	0.165	0.106	1.613	1.015	0.092	362.26	0.869	0.662	1.022	1.473	0.069
343.86	0.187	0.117	1.551	1.023	0.101	364.10	0.894	0.715	1.014	1.463	0.052
344.12	0.203	0.127	1.549	1.023	0.107	365.99	0.923	0.777	1.008	1.493	0.038
344.24	0.215	0.132	1.512	1.029	0.111	367.38	0.943	0.829	1.008	1.509	0.031
344.33	0.221	0.136	1.504	1.031	0.114	368.21	0.952	0.854	1.004	1.482	0.023
344.50	0.235	0.142	1.472	1.036	0.118	369.04	0.963	0.887	1.004	1.490	0.018
344.82	0.254	0.154	1.456	1.039	0.124	369.76	0.974	0.920	1.008	1.462	0.018
345.10	0.274	0.165	1.431	1.045	0.130	370.45	0.981	0.939	1.001	1.519	0.009
345.64	0.303	0.183	1.411	1.048	0.137	370.75	0.985	0.950	1.000	1.514	0.006
345.91	0.331	0.193	1.349	1.070	0.144	370.93	0.987	0.958	1.000	1.556	0.006
346.79	0.376	0.219	1.308	1.082	0.150	371.07	0.989	0.963	1.000	1.569	0.005
347.42	0.421	0.238	1.240	1.118	0.155	372.09	1.000	1.000	1.000		0.000
					ethyl propanoate (1) + octane (2)						
398.82	0.000	0.000		1.000	0.000	376.06	0.580	0.735	1.128	1.204	0.148
396.92	0.023	0.069	1.517	1.002	0.012	375.73	0.598	0.747	1.123	1.214	0.147
396.40	0.030	0.086	1.505	1.004	0.016	375.45	0.629	0.757	1.091	1.272	0.144
395.97	0.034	0.099	1.524	1.006	0.020	375.22	0.644	0.767	1.086	1.282	0.141
395.47	0.041	0.116	1.492	1.008	0.024	375.09	0.649	0.771	1.087	1.283	0.142
394.60	0.053	0.146	1.501	1.009	0.030	375.06	0.658	0.775	1.078	1.298	0.138
393.96	0.061	0.168	1.522	1.009	0.034	374.62	0.688	0.793	1.068	1.328	0.134
392.41	0.086	0.218	1.458	1.016	0.047	374.46	0.702	0.801	1.062	1.345	0.130
391.13	0.107	0.259	1.434	1.021	0.057	374.32	0.715	0.808	1.057	1.358	0.127
389.32	0.140	0.320	1.428	1.022	0.068	374.16	0.730	0.816	1.050	1.381	0.123
388.54	0.151	0.341	1.435	1.026	0.076	373.99	0.747	0.825	1.042	1.409	0.118
387.78	0.166	0.363	1.417	1.031	0.083	373.83	0.763	0.834	1.036	1.436	0.113
387.23	0.178	0.381	1.402	1.034	0.088	373.69	0.777	0.843	1.032	1.453	0.108
386.70	0.189	0.397	1.402	1.035	0.091	373.54	0.793	0.853	1.027	1.475	0.102
386.09	0.202	0.416	1.391	1.038	0.097	373.40	0.809	0.862	1.023	1.500	0.095
385.40	0.216	0.435	1.388	1.042	0.103	373.23	0.830	0.873	1.015	1.555	0.088
384.68	0.239	0.459	1.350	1.049	0.108	373.10	0.845	0.884	1.013	1.574	0.081
382.59	0.292	0.518	1.321	1.067	0.127	372.92	0.866	0.897	1.008	1.626	0.072
381.94	0.311	0.538	1.308	1.073	0.132	372.81	0.880	0.906	1.006	1.647	0.065
380.88	0.352	0.574	1.268	1.086	0.137	372.71	0.893	0.916	1.004	1.674	0.059
380.30	0.369	0.588	1.261	1.095	0.143	372.59	0.910	0.927	1.001	1.728	0.050
379.71	0.395	0.610	1.241	1.102	0.144	372.52	0.924	0.937	0.999	1.765	0.042
379.47	0.407	0.619	1.231	1.105	0.144	372.44	0.937	0.947	0.997	1.814	0.035
379.14	0.422	0.630	1.219	1.113	0.146	372.38	0.947	0.955	0.997	1.831	0.029
378.74	0.439	0.643	1.207	1.122	0.147	372.34	0.957	0.962	0.996	1.873	0.023
378.33	0.460	0.656	1.191	1.134	0.149	372.29	0.967	0.970	0.995	1.933	0.017
377.96	0.481	0.668	1.171	1.153	0.150	372.26	0.974	0.977	0.994	1.965	0.012
377.60	0.500	0.681	1.160	1.163	0.150	372.22	0.982	0.983	0.994	2.026	0.007
377.16	0.522	0.694	1.148	1.181	0.151	372.20	0.987	0.987	0.994	2.085	0.004
376.90	0.536	0.704	1.141	1.189	0.151	372.18	0.992	0.992	0.994	2.177	0.000
376.65	0.551	0.713	1.132	1.201	0.150	372.09	1.000	1.000	1.000		0.000
376.42	0.560	0.721	1.135	1.196	0.150						
					methyl butanoate (1) + hexane (2)						
341.82	0.000	0.000		1.000	0.000	346.02	0.314	0.170	1.452	1.071	0.164
341.93	0.011	0.008	2.382	1.000	0.009	346.63	0.349	0.185	1.393	1.088	0.171
341.96	0.016	0.012	2.365	1.000	0.013	346.90	0.370	0.192	1.350	1.105	0.174
342.03	0.022	0.016	2.301	1.000	0.018	347.34	0.391	0.203	1.322	1.116	0.176
342.10	0.029	0.021	2.221	1.001	0.024	347.82	0.413	0.216	1.309	1.123	0.179

Table 3. continued

T (K)	x_1	y_1	γ_1	γ_2	g^E/RT	T (K)	x_1	y_1	γ_1	γ	g^E/RT
					methyl butanoate (1) + hexane (2)						
342.21	0.037	0.025	2.157	1.000	0.029	348.13	0.433	0.224	1.280	1.141	0.181
342.28	0.043	0.030	2.194	1.000	0.033	348.34	0.440	0.229	1.279	1.139	0.181
342.34	0.046	0.032	2.150	0.999	0.035	348.71	0.455	0.237	1.264	1.147	0.181
342.37	0.050	0.033	2.080	1.001	0.037	349.20	0.480	0.248	1.231	1.168	0.181
342.38	0.051	0.035	2.103	1.001	0.039	350.13	0.517	0.271	1.206	1.189	0.180
342.45	0.058	0.039	2.072	1.002	0.044	350.57	0.547	0.282	1.165	1.233	0.179
342.60	0.070	0.046	2.004	1.003	0.052	350.93	0.559	0.289	1.156	1.241	0.176
342.80	0.087	0.056	1.965	1.004	0.062	351.29	0.576	0.299	1.146	1.258	0.176
342.96	0.098	0.063	1.953	1.004	0.069	352.93	0.629	0.336	1.110	1.305	0.164
343.08	0.109	0.068	1.895	1.007	0.076	354.90	0.685	0.382	1.081	1.355	0.149
343.25	0.123	0.076	1.854	1.010	0.085	355.95	0.716	0.407	1.063	1.399	0.139
343.51	0.142	0.087	1.808	1.013	0.095	356.87	0.731	0.428	1.059	1.394	0.131
343.62	0.154	0.091	1.745	1.019	0.101	357.89	0.756	0.454	1.049	1.427	0.123
343.67	0.156	0.094	1.772	1.016	0.103	359.00	0.782	0.481	1.035	1.473	0.111
343.67	0.157	0.092	1.730	1.020	0.103	361.32	0.822	0.543	1.026	1.500	0.094
343.76	0.163	0.096	1.735	1.020	0.106	364.34	0.868	0.625	1.014	1.531	0.069
343.87	0.172	0.102	1.736	1.021	0.111	366.30	0.891	0.683	1.014	1.492	0.056
344.10	0.182	0.108	1.724	1.019	0.115	367.20	0.904	0.711	1.011	1.511	0.050
344.32	0.202	0.117	1.658	1.028	0.125	369.62	0.934	0.789	1.007	1.515	0.034
344.55	0.219	0.124	1.612	1.035	0.132	371.49	0.956	0.852	1.003	1.518	0.022
344.76	0.237	0.131	1.568	1.044	0.139	373.18	0.974	0.914	1.004	1.415	0.014
344.95	0.249	0.137	1.542	1.048	0.143	374.37	0.985	0.950	0.996	1.447	0.001
345.20	0.268	0.145	1.501	1.058	0.150	374.75	0.990	0.966	0.996	1.454	0.000
345.49	0.288	0.154	1.465	1.067	0.156	374.99	0.992	0.972	0.994	1.426	−0.004
345.70	0.295	0.160	1.479	1.063	0.158	375.74	1.000	1.000	1.000		0.000
					methyl butanoate (1) + octane (2)						
398.82	0.000	0.000		1.000	0.000	376.95	0.696	0.775	1.068	1.373	0.142
398.46	0.006	0.015	1.390	1.000	0.002	376.83	0.707	0.784	1.067	1.374	0.139
398.18	0.010	0.026	1.392	1.001	0.004	376.67	0.725	0.796	1.060	1.393	0.133
397.45	0.021	0.052	1.375	1.003	0.010	376.57	0.746	0.805	1.044	1.450	0.127
396.31	0.038	0.094	1.420	1.006	0.019	376.40	0.762	0.816	1.042	1.465	0.122
396.28	0.038	0.093	1.412	1.008	0.020	376.28	0.776	0.824	1.037	1.492	0.118
395.63	0.048	0.117	1.424	1.009	0.026	376.23	0.791	0.833	1.030	1.524	0.111
394.83	0.061	0.145	1.403	1.013	0.033	376.19	0.812	0.848	1.023	1.536	0.099
393.24	0.089	0.203	1.410	1.015	0.044	376.13	0.825	0.857	1.019	1.557	0.093
390.20	0.142	0.301	1.412	1.029	0.073	376.03	0.838	0.867	1.017	1.578	0.088
388.20	0.187	0.367	1.382	1.039	0.091	375.96	0.853	0.877	1.013	1.610	0.081
386.41	0.229	0.424	1.368	1.049	0.108	375.92	0.867	0.886	1.009	1.641	0.074
385.10	0.263	0.465	1.350	1.058	0.121	375.89	0.881	0.897	1.005	1.675	0.065
383.15	0.332	0.529	1.285	1.087	0.139	375.81	0.897	0.908	1.003	1.715	0.058
382.00	0.383	0.575	1.246	1.102	0.144	375.75	0.908	0.918	1.002	1.737	0.052
381.42	0.408	0.592	1.224	1.120	0.150	375.75	0.922	0.928	0.998	1.791	0.043
380.55	0.449	0.622	1.199	1.144	0.155	375.70	0.933	0.937	0.998	1.803	0.038
379.79	0.489	0.649	1.174	1.170	0.159	375.65	0.945	0.948	0.997	1.857	0.031
379.16	0.526	0.673	1.152	1.197	0.160	375.63	0.958	0.959	0.996	1.887	0.023
378.65	0.557	0.694	1.137	1.219	0.159	375.60	0.966	0.967	0.996	1.928	0.018
378.32	0.582	0.707	1.119	1.250	0.159	375.59	0.974	0.974	0.996	1.956	0.014
378.06	0.606	0.720	1.103	1.277	0.156	375.60	0.981	0.981	0.996	1.981	0.009
377.64	0.633	0.736	1.092	1.310	0.155	375.61	0.988	0.987	0.995	2.046	0.004
377.37	0.656	0.751	1.084	1.329	0.150	375.62	0.993	0.993	0.995	2.129	0.000
377.13	0.678	0.764	1.075	1.352	0.146	375.63	0.997	0.997	0.994	2.392	−0.003
377.04	0.688	0.773	1.074	1.348	0.143	375.74	1.000	1.000	1.000		0.000
					ethyl butanoate (1) + hexane (2)						
341.82	0.000	0.000		1.000	0.000	353.55	0.450	0.145	1.183	1.112	0.134
342.01	0.005	0.002	2.093	0.998	0.001	354.29	0.471	0.153	1.164	1.123	0.133
342.16	0.015	0.005	1.898	1.000	0.010	355.61	0.506	0.170	1.146	1.138	0.133
342.34	0.024	0.008	1.897	1.001	0.016	357.78	0.554	0.198	1.129	1.148	0.129
342.68	0.038	0.012	1.812	1.001	0.023	361.33	0.642	0.246	1.067	1.226	0.114
343.00	0.052	0.017	1.793	1.001	0.031	362.79	0.673	0.267	1.052	1.256	0.109
343.46	0.074	0.023	1.701	1.005	0.044	364.34	0.702	0.290	1.038	1.285	0.101
343.95	0.092	0.029	1.666	1.005	0.051	367.85	0.755	0.348	1.028	1.315	0.088
344.52	0.117	0.037	1.619	1.008	0.063	369.08	0.773	0.369	1.023	1.334	0.083

Table 3. continued

T (K)	x_1	y_1	γ_1	γ_2	g^E/RT	T (K)	x_1	y_1	γ_1	γ	g^E/RT
					ethyl butanoate (1) + hexane (2)						
345.05	0.137	0.043	1.587	1.009	0.071	373.37	0.824	0.450	1.019	1.351	0.068
345.46	0.158	0.048	1.536	1.015	0.080	375.15	0.843	0.485	1.014	1.360	0.060
345.93	0.171	0.054	1.542	1.012	0.083	379.98	0.894	0.592	1.004	1.430	0.042
346.21	0.192	0.058	1.457	1.026	0.093	381.95	0.909	0.641	1.007	1.405	0.037
346.63	0.204	0.063	1.465	1.023	0.096	383.07	0.919	0.668	1.004	1.417	0.032
347.01	0.220	0.067	1.437	1.028	0.101	384.24	0.929	0.699	1.003	1.436	0.029
347.48	0.241	0.073	1.397	1.036	0.108	388.12	0.955	0.807	1.004	1.349	0.017
348.01	0.267	0.079	1.337	1.050	0.113	390.12	0.972	0.866	1.001	1.413	0.010
349.46	0.322	0.096	1.273	1.069	0.123	391.19	0.979	0.900	1.001	1.410	0.008
350.00	0.334	0.102	1.279	1.065	0.124	392.30	0.986	0.935	1.001	1.330	0.005
350.64	0.354	0.110	1.276	1.068	0.129	393.37	0.994	0.971	1.001	1.336	0.003
351.19	0.376	0.117	1.246	1.080	0.131	394.31	1.000	1.000	1.000		0.000
352.34	0.419	0.130	1.193	1.108	0.133						
					ethyl butanoate (1) + octane (2)						
398.82	0.000	0.000		1.000	0.000	392.11	0.591	0.599	1.077	1.176	0.110
398.30	0.017	0.026	1.379	1.004	0.010	392.10	0.605	0.610	1.071	1.186	0.109
398.07	0.026	0.039	1.376	1.006	0.014	392.09	0.621	0.622	1.065	1.196	0.107
397.57	0.052	0.076	1.362	1.006	0.022	392.06	0.637	0.635	1.060	1.208	0.106
396.71	0.089	0.130	1.369	1.010	0.037	392.08	0.649	0.645	1.056	1.214	0.104
396.39	0.104	0.151	1.372	1.010	0.042	392.08	0.662	0.655	1.053	1.223	0.102
396.08	0.121	0.172	1.355	1.013	0.048	392.09	0.676	0.667	1.049	1.233	0.100
395.75	0.139	0.195	1.353	1.014	0.054	392.10	0.693	0.680	1.043	1.249	0.098
395.42	0.159	0.216	1.320	1.020	0.061	392.11	0.706	0.692	1.040	1.260	0.096
395.14	0.174	0.236	1.329	1.019	0.065	392.13	0.721	0.704	1.037	1.272	0.093
394.88	0.193	0.256	1.310	1.023	0.070	392.17	0.737	0.718	1.033	1.285	0.090
394.61	0.213	0.278	1.297	1.026	0.076	392.21	0.754	0.733	1.028	1.303	0.086
394.32	0.233	0.299	1.283	1.031	0.081	392.38	0.792	0.767	1.020	1.335	0.076
394.10	0.251	0.317	1.271	1.034	0.085	392.43	0.802	0.776	1.018	1.348	0.073
393.95	0.265	0.331	1.264	1.036	0.088	392.51	0.816	0.789	1.015	1.361	0.069
393.76	0.282	0.346	1.250	1.041	0.092	392.58	0.828	0.801	1.014	1.371	0.066
393.56	0.304	0.367	1.230	1.048	0.096	392.65	0.841	0.814	1.013	1.382	0.062
393.36	0.328	0.386	1.209	1.058	0.100	392.73	0.852	0.826	1.011	1.395	0.058
392.87	0.392	0.440	1.169	1.080	0.108	392.81	0.864	0.837	1.009	1.412	0.054
392.72	0.421	0.464	1.152	1.091	0.110	392.90	0.876	0.849	1.007	1.428	0.050
392.56	0.451	0.487	1.133	1.106	0.112	393.01	0.888	0.862	1.005	1.444	0.046
392.51	0.464	0.499	1.129	1.109	0.112	393.11	0.899	0.874	1.004	1.456	0.041
392.44	0.475	0.506	1.123	1.116	0.113	393.30	0.920	0.898	1.002	1.484	0.034
392.40	0.485	0.515	1.121	1.118	0.113	393.56	0.942	0.924	0.999	1.529	0.024
392.34	0.501	0.527	1.110	1.129	0.113	393.66	0.950	0.934	0.999	1.542	0.020
392.27	0.518	0.539	1.101	1.141	0.114	393.82	0.962	0.949	0.998	1.551	0.015
392.24	0.531	0.552	1.100	1.142	0.113	393.98	0.975	0.965	0.998	1.569	0.009
392.18	0.549	0.564	1.090	1.156	0.113	394.13	0.986	0.980	0.997	1.613	0.004
392.16	0.565	0.578	1.086	1.160	0.111	394.31	1.000	1.000	1.000		0.000
392.13	0.579	0.589	1.080	1.170	0.111						

although its effect is moderate and the error can be accepted.

(b) The *areas-test*[50] establishes a value for the parameter $D_A <$ 2% to define the global consistency. According to this, the systems studied here are all inconsistent, see Table 4. The greatest deviation for D_A corresponds to the binary methyl propanoate + octane, Figure S4.1, which is associated with the maximum of γ_1 mentioned previously.

(c) The *Fredenslund test*[51] uses the residual value of the vapor composition as an index of quality of the VLE data, as individually as jointed. All the systems are below the limit established $\overline{\delta}y_1 < 0.01$ and are, therefore, considered to be consistent; see Table 4. However, some deficiencies are also observed: there is no a random distribution of δy_1, this means inconsistency for the binary ethyl propanoate (1) + hexane (2), with many points in $x_1 > 0.2$ that exceed the established limit, and for the binary ethyl butanoate + octane, Figure S4.2, with a region $0.5 > x_1 > 0.2$, of clear inconsistency. In spite of this, the overall value $\overline{\delta}y_1$ satisfies the limiting condition.

(d) *Wisniak test*,[52] verifies all systems, even with the most restrictive limiting condition, $D_W < 3$. Figure S4.3 shows the individual values for the parameter L_i/W_i for the system methyl propanoate+octane, which presents the highest global error. A more detailed look confirms that most of the data satisfy the limit established of $0.92 < L_i/W_i < 1.08$.

(e) *Kojima test*,[53] validates half of the systems, but there is not a clear reason for the solutions rejected. Figure S4.4 represents the curves used to calculate the I_i of the binary ethyl propanoate(1)+hexane(2), which presents the poorest results. In this figure, $\ln(\gamma_2/\gamma_1)$ does not coincide well with
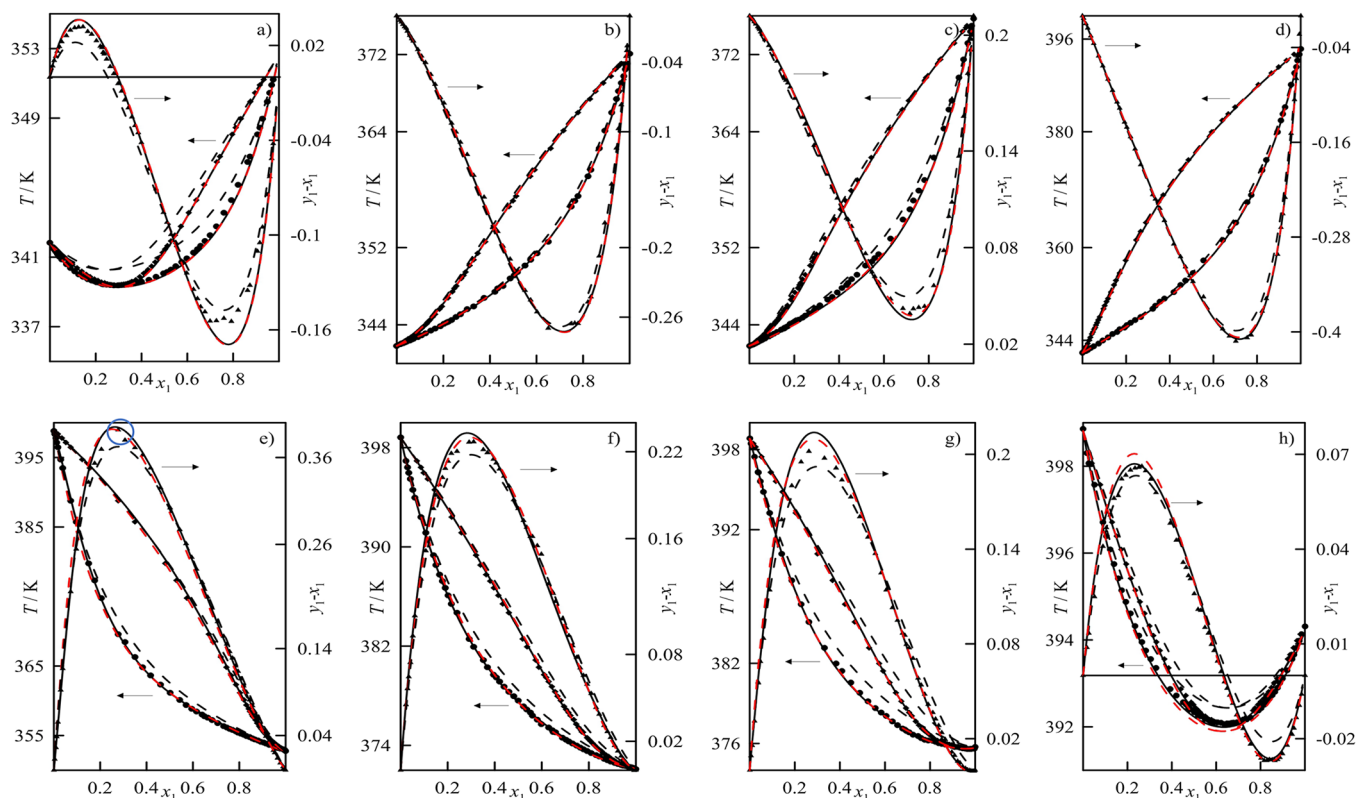
Figure 5. Plot of iso-101.32 kPa VLE for: (a) methyl propanoate (1) + hexane (2), (b) ethyl propanoate (1) + hexane (2), (c) methyl butanoate (1) + hexane (2), (d) ethyl butanoate (1) + hexane (2), (e) methyl propanoate (1) + octane (2), (f) ethyl propanoate (1) + octane (2), (g) methyl butanoate (1) + octane (2), (h) ethyl butanoate (1) + octane (2). (♦) T vs y_1 (●) T vs x_1 (▲) $(y_1 - x_1)$ vs x_1. (—) Modeling with proposed model, eqs 19 and 20), (dashed line) estimated by UNIFAC, (red dashed line) by NRTL.

g^E/RTx_1x_2 when $x_1 \to 1$, mainly owing to an anomalous behavior of adimensional Gibbs function at $x_1 > 0.8$, which is also observed to a lesser extent in $\ln(\gamma_2/\gamma_1)$. However, the coherence between g^E/RTx_1x_2 and $\ln(\gamma_2/\gamma_1)$ when $x_1 \to 1$ is acceptable.

(f) *Direct Van Ness test*[54] verifies all the binaries of this work. The values observed for the deviation $s[\ln(\gamma_1/\gamma_2)]$ are lower than the limits established by Van Ness. Figure S4.5 shows the residues $\delta[\ln(\gamma_1/\gamma_2)]$ for the binary methyl propanoate + octane, which presents the greatest index. In spite of that the global deviation s complies with the limits established by Van Ness, the distribution of the residues observed in Figure S4.5 reflects some consistency problems associated with an incoherence between g^E and the activity coefficients.

Application of these five methods validates the most of the systems studied here. Only the areas-test, which is highly exacting, invalidates all the systems and Kojima's test, which invalidates four of the eight systems, find problems with the quality of the experimental iso-*p* VLE points.

3.3.1.1. Application of a New Method To Check iso-p VLE Data. For the first time in the thermodynamic exploration of new VLE data, a method published recently[27,55] is used to analyze the consistency of the data. Due to the thermodynamic–mathematical rigor of this approach, we consider it convenient to make some observations concerning its application, so it can be fully understood by other investigators. The method is based on the assumption that the validation of experimental data obtained in phase equilibria must be carried out according to procedures that satisfy resolution of the Gibbs–Duhem equation.

$$\sum_{i=1}^{n} x_i d \ln \gamma_i = \frac{v^E}{RT} dp - \frac{h^E}{RT^2} dT \tag{11}$$

The differential of γ_i is generated from eq 9. To avoid extend the development of eq 11, we consider the particular case of a binary, and is expressed for iso-*p* VLE, as

$$\left[\frac{y_1 - x_1}{y_1(1 - y_1)} - \sum_{i=1}^{2} \left(\frac{\partial \ln \Phi_i}{\partial y_1} \right)_{T,p} \right] dy_1 = \varphi_T dT \quad i = 1, 2 \tag{12}$$

Where:

$$\varphi_T = \left[\frac{h^E}{RT^2} - \sum_{i=1}^{2} x_i \left(\frac{\partial \ln p_i^o}{\partial T} \right) + \sum_{i=1}^{2} x_i \left(\frac{\partial \ln \Phi_i}{\partial T} \right) \right]_{p,x} \tag{13}$$

Φ_i was established in section 3.3. Equations 12 and 13 show other thermodynamic–mathematical approaches to the Gibbs–Duhem equation, already adapted to iso-*p* VLE studies. Its resolution is proposed by two different ways which we refer as *differential-form* and *integral-form* of the consistency test, and by applying both procedures the investigator verifies the quality of experimental VLE data. The *differential-form* verifies the thermodynamic consistency through the compositions, using eq 12, which gives two relationships:

$$\zeta_{i,\exp} = \frac{y_1 - x_1}{y_1 1 - y_1)}$$

$$\zeta_{i,cal} = \sum_{i=1}^{2} \left(\frac{\partial \ln \Phi_i}{\partial y_1} \right)_{T,p} + \varphi_T \left(\frac{dT}{dy_1} \right) \tag{14}$$
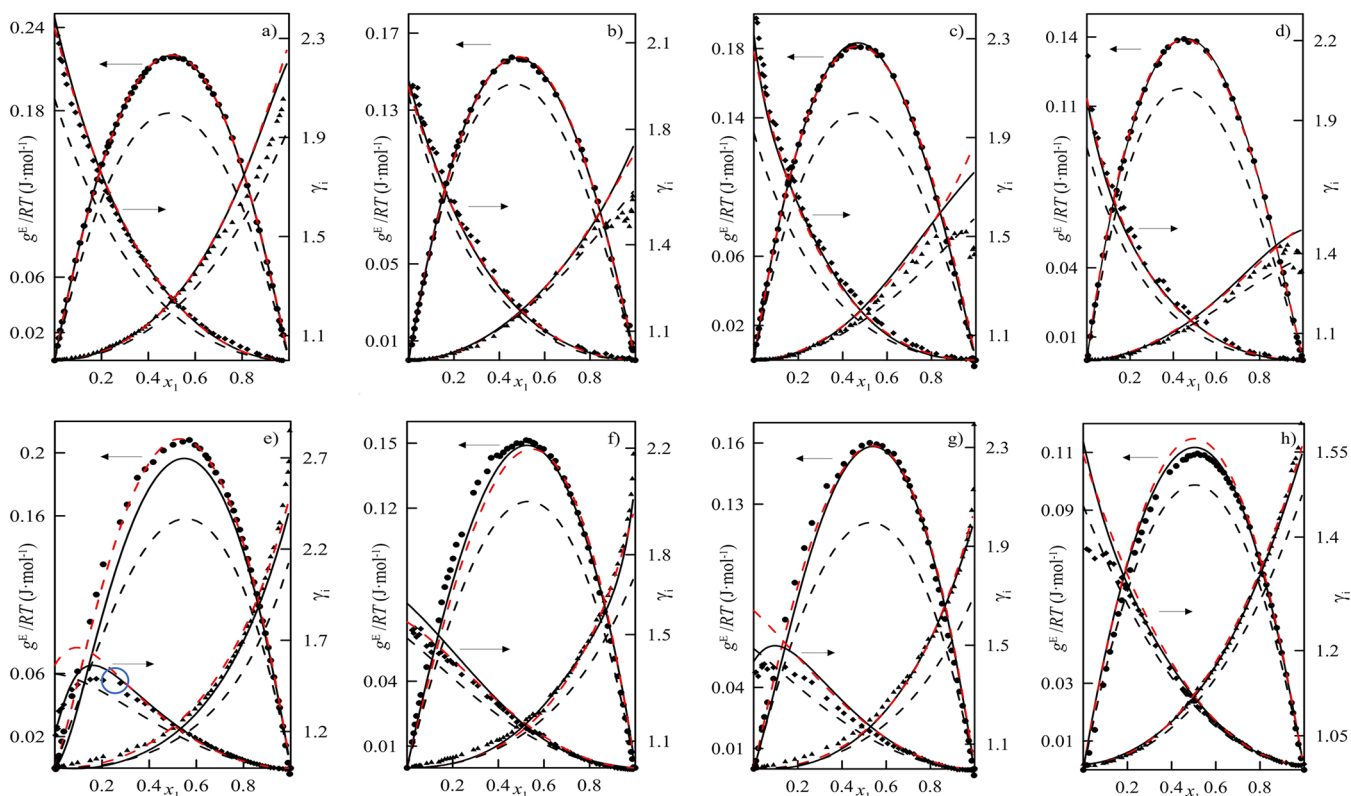
Figure 6. Properties for iso-101.32 kPa VLE of (a) methyl propanoate (1) + hexane (2), (b) ethyl propanoate (1) + hexane (2), (c) methyl butanoate (1) + hexane (2), (d) ethyl butanoate (1) + hexane (2), (e) methyl propanoate (1) + octane (2), (f) ethyl propanoate (1) + octane (2), (g) methyl butanoate (1) + octane (2), (h) ethyl butanoate (1) + octan e(2). (●) g^E/RT vs x_1, (♦) γ_1 vs x_1, (▲)γ_2 vs x_1. (—) Modeling with proposed model, eqs 19 and 20), (dashed line) estimated by UNIFAC, (red dashed line) by NRTL.

Table 4. Results Obtained in the Application of Different Consistency Tests[a]

	area test		Fredenslund test		Wisniak test		Kojima test		Van Ness test		proposed test		
system	D_A	V	$100 \cdot \overline{\delta} y_1$	V	D_W	V	$M(I_i)$	V	$\delta[\ln(\gamma_1/\gamma_2)]$	V	$\overline{\delta}T$	$\overline{\delta}\xi_i$	V
methyl propanoate (1) + hexane (2)	7	nv	0.7	v	0.8	v	5	v	0.03	v	0.1	0.030	v
methyl propanoate (1) + octane (2)	24	nv	0.8	v	3.0	v	58	nv	0.10	v	0.1	0.004	v
ethyl propanoate (1) + hexane (2)	19	nv	0.8	v	1.1	v	68	nv	0.09	v	0.2	0.000	v
ethyl propanoate (1) + octane (2)	13	nv	0.5	v	2.3	v	18	v	0.05	v	0.1	0.018	v
methyl butanoate (1) + hexane (2)	15	nv	0.6	v	1.3	v	64	nv	0.07	v	0.4	0.003	v
methyl butanoate (1) + octane (2)	19	nv	0.6	v	1.9	v	18	v	0.05	v	0.1	0.004	v
ethyl butanoate (1) + hexane (2)	19	nv	0.4	v	2.1	v	32	nv	0.08	v	0.3	0.000	v
ethyl butanoate (1) + octane (2)	12	nv	0.3	v	1.0	v	24	v	0.02	v	0.1	0.017	v

[a]Limit values established for each of them: areas test, $D_A < 2$; Fredenslund test, $100 \cdot \overline{\delta} y_1 < 1$; Wisniak test, $D_W < 3$; Kojima test, $M(I_i) < 30$; Van Ness test, $s(\ln \gamma_1/\gamma_2) < 0.16$; proposed test, $\overline{\delta}T < 2$, $s(\delta T) < 0.2$; $\overline{\delta}\zeta_i < 5$, $s(\delta\zeta_i) < 0.2$. V: validation; v: verify; nv: non-verify; $M(I_i)$, maximum value between I_1 and I_2.

The first contains the experimental data (x_i, y_i) obtained from **experimentation** and the second requires a previous **modeling** step. For both of these, a parameter ζ is defined, assigned respectively, to quasi-direct experimentation and to experimentation-modeling, whose difference corresponds to point-to-point and global inconsistency index, defined respectively, by

$$\delta\zeta_{i,j} = |\zeta_{1,j,exp} - \zeta_{1,j,cal}|\overline{\delta}\zeta_i = \sum_{j=1}^{m} \delta\zeta_{i,j}/m$$

$$m = \text{no. of exptl points} \tag{15}$$

In the *integral-form* temperature values are calculated, which are compared with experimental values in order to validate the relation between this variable and the composition at each point j, $(T_j - x_{1,j})$, by the residual:

$\delta T_j = |T_{j,exp} - T_{j,cal}|$ and the global one for the data series

$$\overline{\delta}T = \sum_{j=1}^{m} \delta T_j/m \tag{16}$$

Allowable limit values for the averages of the parameters, $\overline{\delta}\zeta$ and $\overline{\delta}T$, defined by eqs 15 and 16, respectively, are:

$$\frac{100\overline{\delta}T}{[\max(T_{k,exp}) - \min(T_{k,exp})]} < 2$$

$$\text{and } \frac{100\overline{\delta}\zeta}{[\max(\zeta_{k,exp}) - \min(\zeta_{k,exp})]} < 5 \tag{17}$$

Nonetheless, the mean values of the corresponding inconsistency functions are insufficient to guarantee the validity of the

data. This is because this statistic does not provide information about whether the distribution of errors is random or systematic, or if these errors are accumulated in a specific region of the diagram. Therefore, the information about the errors is completed with the standard deviations, s, of the specific residuals defined by

$$s(\delta T) = \left[\sum_j (\delta T_j - \bar{\delta}T)^2 / m \right]^{0.5} \quad \text{and}$$

$$s(\delta \zeta) = \left[\sum_j (\delta \zeta_j - \bar{\delta}\zeta)^2 / m \right]^{0.5} \tag{18}$$

for which the maximum permitted value is fixed as 0.2 for both statistical indices.

The method described is applied to the systems studied here using the parameters of the model obtained as described below. The resulting values for the *integral-form* and the *differential-form* of the test, and the global assessmenta of the method are recorded in Table 4 and all show a positive consistency. Some examples are explained in detail below. The highest degree of inconsistency, according to the *integral-form* of the test, is obtained with the solution of methyl propanoate (1) + hexane (2). For this system, the residuals functions, eqs 16 and 17, are shown in Figure 7, observing that, at $x_1 > 0.7$ values above the limit
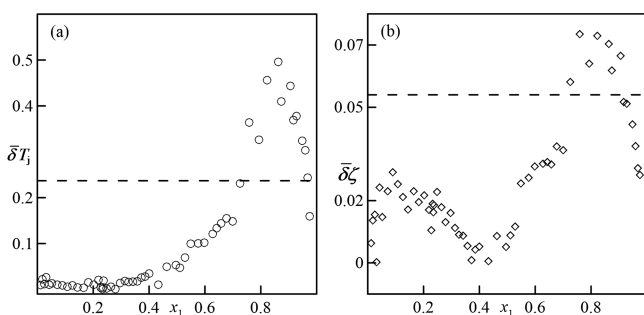
Figure 7. Results obtained by applying the consistency-test proposed to the binary methyl propanoate (1) + hexane (2). (a) *integral-form*: (O) residuals, eq 16; (b) *differential-form*: (◊) residuals, eq 17. (– – –) consistency limit line.

established by eqs 18 are obtained for the data set. This result is important for the *integral-form*, since some points reach as high as twice this limit. However, the set of results is positively valued and the data series is consistent.

The least favorable result for the *differential-form* occurs for the solution of methyl butanoate (1)+hexane (2), for which the residuals are shown in Figure 8. In this case, the *integral-form* produces some highly favorable results, with only three values exceeding the inconsistency limit, see Figure 8(a). However, the *differential-form*, Figure 8(b), presents a large amount of inconsistent data, especially in the hydrocarbon rich region. The errors observed are clearly random, which explains why the parameter $s(\delta \zeta)$, has acceptable values. On the whole, this series is also consistent.

The results obtained with the different classical consistency tests used, and the new method proposed by the authors,[27,55] qualify the iso-p VLE data to be of a sufficient quality. These experimental data can, therefore, be considered to be suitable for use in calculations of chemical engineering processes, such as the simulation/design of separation equipment.
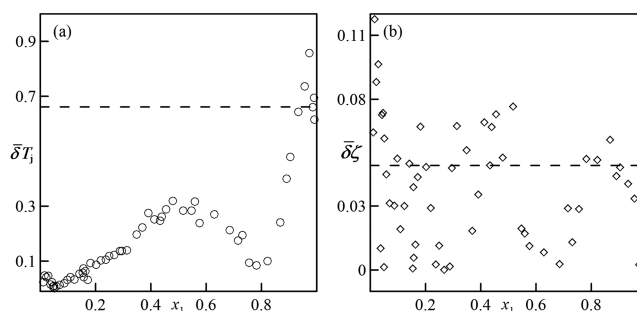
Figure 8. Results obtained by applying the consistency test proposed to the binary methyl butanoate (1) + hexane (2). (a) *integral-form*: (O) residuals, eq 16; (b) *differential-form*: (◊) residuals, eq 17. (– – –) consistency limit line.

4. COMBINED MATHEMATICAL TREATMENT OF VALIDATED DATA. CORRELATION AND PREDICTION

Modeling of properties of energetic nature (iso-p VLE, h^E, c_p^E) obtained experimentally in this work is carried out in a combined correlation process, taking into consideration the thermodynamic formal relationships. The v^E have been omitted owing to a lack of data for $g^E = g^E(p)$. A model, similar to that established by eq 2, was used but adapted to excess Gibbs function g^E

$$g^E = z_1 z_2 \sum_{i=0}^{2} y_i z_1^i = z_1 (1 - z_1)(g_0 + g_1 z_1 + g_2 z_1^2) \tag{19}$$

where $g_i = g_i(p,T)$. A new relationship is then established, as an extension of eq 3, which gives acceptable results in the operation proposed:

$$g_i = G_{i1} + G_{i2} p^2 + G_{i3} pT + \frac{G_{i4}}{T} + G_{i5} T^2 \tag{20}$$

With eqs 19 and 20, other functionals are obtained for h^E and c_p^E:

$$h^E = z_1 (1 - z_1) \sum_{i=0}^{2} \left(G_{i1} + G_{i2} p^2 + \frac{2 G_{i4}}{T} - G_{i5} T^2 \right) z_1^i \tag{21}$$

$$c_p^E = -z_1 (1 - z_1) \sum_{i=0}^{2} \left(\frac{2 G_{i4}}{T^2} + 2 G_{i5} T \right) z_1^i \tag{22}$$

and the activity coefficients γ_i

$$RT \ln \gamma_i = z_1 (1 - z_1) \sum_{j=0}^{2} g_j z_1^j + (2 - i - x_1)$$
$$\left[\sum_{j=0}^{3} (j+1)(g_j - g_{j-1}) z_1^j \right] k_g \left(\frac{z_1}{x_1} \right)^2 \tag{23}$$

where $g_{-1} = g_3 = 0$. In the special case in which $x_i \rightarrow 0$, expressions for these activity coefficients at infinite dilution are calculated

$$\ln \gamma_1^\infty \equiv \lim_{x_1 \rightarrow 0} \gamma_1 = \frac{g_0}{k_g RT_{b,2}^o};$$

$$\ln \gamma_2^\infty \equiv \lim_{x_2 \rightarrow 0} \gamma_2 = \frac{k_g (g_0 + g_1 + g_2)}{RT_{b,1}^o} \tag{24}$$

where now k_g is a parameter obtained from the fitting of iso-p VLE data. The parameter "k_Y" defined for the individual

correlation of mixing properties (h^E, v^E and c_p^E) see eqs 6 and 7, is not adequate when a combined correlation of all the properties is carried out, especially considering VLE values. To date, it has not been possible to establish a scientific definition for k_g. For this reason, a multiproperty correlation was carried out with eqs 19−24, using two optimization techniques to obtain the best representations, and using a genetic algorithm (GA) as a searching tool in both cases. As we had our own data for c_p^E, in this work a stepwise fitting procedure was used (step-by-step optimization, SSO), minimizing a single property at each step, in addition to the multiobjective optimization, MOO, used in other works.[4,22,24] In this latter procedure a global objective function is established of the form

$$OF(G_{i1},\ G_{i2},\ G_{i3},\ G_{i4},\ G_{i5},\ k_c,\ k_h,\ k_g)$$
$$= \sum_j c_j s(y_j^E)\ \text{with}\ y^E = \{\gamma_1,\ \gamma_2,\ h^E,\ c_p^E\} \tag{25}$$

where $s(y_j^E)$ the individual errors for each property defined by eq 4; the c_j are weighting coefficients (different for each objective or property) used to obtain optimum values for the parameters G_{ij}. The procedure establishes values for c_i, optimizing eq 25 with a GA, giving place to one result of between those of the solutions front Repetition of the procedure for different values of c_i produces the corresponding set of results, see Figure S5, finally selecting the one that represents a suitable compromise (minimum deviation) among the different errors of the y^E quantities. However, by using the SSO procedure the global problem is modified leading to minimize a single property, with the OF of eq 4, from among those included in eq 25. This procedure takes advantage of the polynomial nature of the model, eqs 19 to 24, in which terms are eliminated by successive derivations, establishing a sequence of simple correlations. In other words, first data fitting is carried out of (c_p^E, x_1, T), defining the parameters that characterize eq 22, which are incorporated into the model of eq 21 for correlation of the (h^E, x_1, T) data, obtaining the parameters G_{i1}, G_{i2}, and k_h. The final step corresponds to treatment of the iso-p VLE data (γ_i, x_i, T) to define G_{i3} and k_g. Figure 9
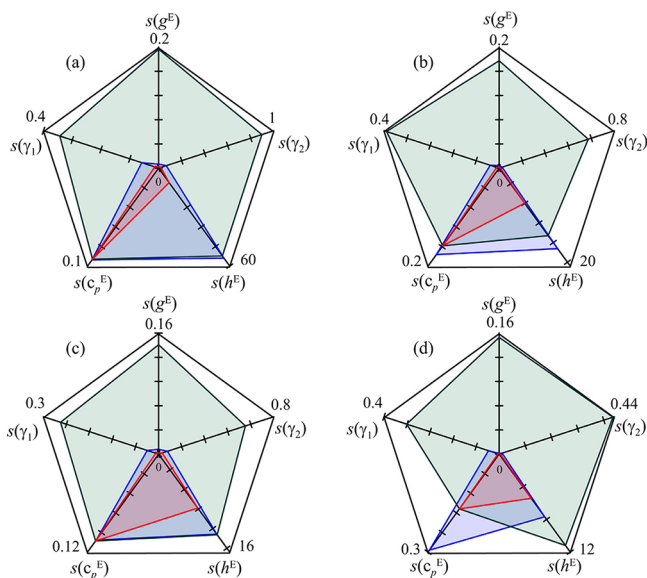
Figure 9. Radar plots for standard deviations resulting in the modeling of the binaries: (a) methyl propanoate + octane, (b) ethyl propanoate + octane, (c) methyl butanoate + octane, and (d) ethyl butanoate + octane: (red zone) the utopic correlacion, (green zone) SSO procedure, and (blue zone) MOO procedure.

represents the error obtained for each of the variables when the data are fitted by the SSO and MOO methods for the four systems containing octane. Analogous representations are also obtained for the solutions with hexane, which we considered unnecessary to reproduce here. The optimal values obtained using both correlation procedures are shown in Table S8. In all cases, the result corresponding to SSO produces the smallest error in c_p^E and the largest error in the iso-p VLE (which is logical considering the successive reduction in the number of parameters during the derivation process). The MOO method however presents smaller errors when reproducing the iso-p VLE but larger ones in the c_p^E, the errors for the h^E are similar for both methods. To summarize the application of both procedures, although the SSO method offers a more thermodynamic sense, the most practical results are achieved by the MOO method when a simultaneous correlation is carried out of all the properties, although this result is not always manifest in the same way. The results obtained by both methods form part of the set of possible solutions that arise when optimizing the objective function. This observation is supported by Figure 10a,b, which shows the projections of the set of results
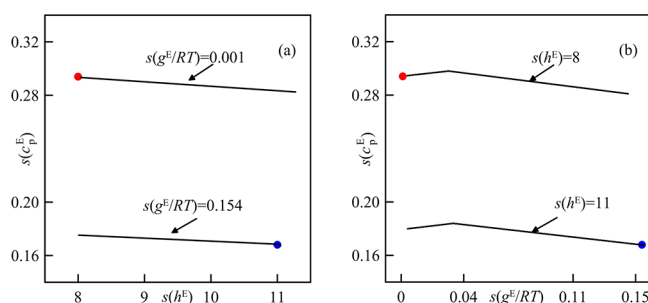
Figure 10. 2D-projection of *Pareto-front* for the binary ethyl butanoate + octane. (a) $s(h^E)$ vs $s(c_p^E)$ at a constant value of $s(g^E/RT)$. (b) $s(g^E/RT)$ vs $s(c_p^E)$ at a constant value of $s(h^E)$. (Red dot) Best result using the MOO procedure. (Blue dot) Best solution using the SSO procedure.

for one of the binaries ethyl butanoate + octane. Figures 5 and 6 depict the curves obtained with the MOO procedure. It can be observed that the model adequately reproduces the equilibrium diagrams, the estimates of h^E and c_p^E shown in Figures S5 and S6 are of sufficient quality.

The NRTL model[25]

$$g^E = RT x_1 x_2 \sum_{i=1}^{2} \sum_{j=1}^{2} \frac{G_{ij}\tau_{ij}}{G_{ij} + x_{ij}}\ \forall\ i \neq j$$

$$G_{ij} = \exp(-\alpha \tau_{ij}) \tag{26}$$

was also applied using an extended expression to establish the dependence of the parameters on temperature, where the parameter τ_{ij} is

$$\tau_{ij} = \Delta g_{ij0} + \frac{\Delta g_{ij1}}{T} + \Delta g_{ij2}\ln T + \Delta g_{ij3}T \tag{27}$$

since the relationship proposed by the commercial software[28] and used by some author[56] did not produce good results. The thermodynamic properties derived from eq 26 are shown in Figure S7. The coefficients Δg_{ij_n}, eq 27, and α, eq 26, were obtained using the same MOO correlation procedure described previously and the values are shown in Table S8 with the deviations by the model for each of the properties. In summary, the model proposed herein gives an acceptable representation of the distribution of experimental data while the NRTL presents slight

Table 5. Activity Coefficients at Infinite Dilution Obtained by a Combined Correlation Procedure and Comparison with Literature Values and Those Estimated by UNIFAC[57]

	methyl propanoate		ethyl propanoate		methyl butanoate		ethyl butanoate	
	hexane	octane	hexane	octane	hexane	octane	hexane	octane
γ_1^∞	2.44	1.38	1.95	1.63	2.14	1.52	1.97	1.40
	2.12[57]	1.64[57]	1.93[1]	1.55[57]	1.93[57]	1.55[57]	1.80[57]	1.48[57]
γ_2^∞	2.04	2.50	1.69	1.96	1.55	2.10	1.41	1.55
	2.03[57]	2.50[57]	1.61[1]	1.83[57]	1.59[57]	1.81[57]	1.357	1.52[57]

discrepancies as observed in Figures 5a−d and 6a−d, for the VLE and in Figures S6 for the h^E. However, estimates of the c_p^E with this model are not good; see Figure S7.

Independently, the experimental behavior of the binaries was estimated with the UNIFAC group contribution method.[57] The method uses the COOC/CH$_2$ interaction parameter pair of the alkanoates with a number of −CH$_2$− groups in the ester acid chain, $u > 2$. Results obtained for the quantities of iso-p VLE (g^E, γ_i, y_i), and for the mixing properties (h^E and c_p^E) are evaluated in Figures 5 and 6 and Figures S6 and S7 giving rise to the following comments. In the diagrams of iso-p VLE (Figures 5 and 6), important differences can be observed relative to experimental data, specifically, the g^E and the γ_i (Figure 6) calculated by UNIFAC are lower than experimental values. Similarly, Table 5 shows that the coefficients at infinite dilution estimated by UNIFAC are lower than experimental values except γ_1^∞ for methyl propanoate (1) + octane (2). The h^E, Figure S5, are also lower than experimental values, while the c_p^E (Figure S6) are not represented at all.

4.1. Azeotropes. Of the eight systems studied, three present azeotropic points ($x_{az,ester}$; T_{az}/K): the binaries methyl propanoate + hexane (0.284; 339.4), methyl butanoate + octane (0.974; 375.6), and ethyl butanoate+octane (0.628; 392.1). The values estimated are compared in Table 6 with those from literature,

Table 6. Experimental Azeotropes for the Binaries an Alkyl Alkanoate (1) + an Alkane (2) and Comparison with Literature Values and Those Predicted by UNIFAC[57] at 101.32 kPa

	$x_{1,az}, T_{az}$ (K)	
mixtures	expt	lit.
methyl propanoate (1) + hexane (2)	0.284, 339.38	0.248, 340.34[57]
		0.216, 339.95[8]
methyl butanoate (1) + octane (2)	0.974, 375.59	zeotropic[8,26]
ethyl butanoate(1)+octane(2)	0.628, 392.06	0.649, 392.43[57]
		0.646, 391.65[8]
		0.605,374.60[7a]

^{a}At $p = 60$ kPa.

revealing some differences in temperature < 0.5 K, but more significant discrepancies in ester composition ($x_{1,exp} − x_{1,lit} \approx 0.07$) for the binary methyl propanoate (1) + hexane (2), which can be justified by the age of the data, which affects the purity of the products. The literature shows the latter of the abovementioned systems to be zeotropic, although, the experimentation reflects the presence of a singular point at $x_{octane} < 0.03$, see Figure 5g. The UNIFAC method does not predict the existence of an azeotropic point for the binary methyl butanoate + octane and the estimation for the other two systems is not very good, with the greatest differences observed in the binary methyl propanoate + hexane, with $|\delta x_{az}| \approx 0.04$ and $|\delta T| \approx 1$ K. Figure 4b shows the situation of the azeotropes obtained in reduced coordinates.

5. REPERCUSSIONS OF THE TRIO EXPERIMENTATION−VERIFICATION−MODELING ON THE SIMULTATION OF A RECTIFICATION PROCESS

When assessing the quality of the experimental data, identifying the nature of the errors along with the modeling stage, is essential in the field of chemical engineering, since the adequate use of the tools used in this work prevents the propagation of errors in the last stage of a process simulation. The basis for engineering design starts with information provided by the experimental stage, as without it, estimation procedures such as UNIFAC[57] are sometimes used but it does not always guarantee the best results, especially in equilibria between phases. Because of this, in this work the highlighted stages are studied, using accurate assessment and representation tools, to verify the degree of error made when comparing the values obtained in the simulation of a rectification process using: (a) estimates by theoretical methods and (b) modeling achieved with real laboratory values. The binary methyl butanoate (1) + octane (2) is chosen to separate in a rectification column whose conditions are previously established. The simulation is carried out with the commercial software AspenPlus and the *Radfrac* block, which performs a rigorous calculus of the equilibrium stages in a column. The following operation values are established, see Figure 11, identical for the two cases proposed above:
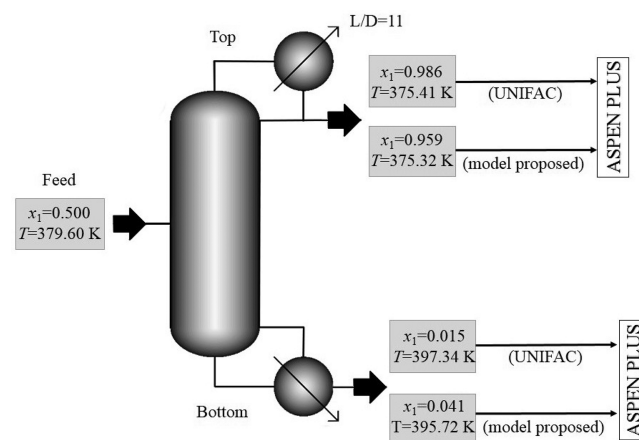
Figure 11. Scheme of the projected rectification column indicating the conditions estimated by the Aspen-Plus simulator using either UNIFAC or the proposed model.

- feed: 1 kmol/h with equimolar composition of saturated liquid at 101.32 kPa
- number of equilibrium stages in column: 40
- feeding stage: 32
- reflux ratio: 11

Figure 12 shows the composition profiles x_{ester} and temperature T versus the number of stages for the simulation performed
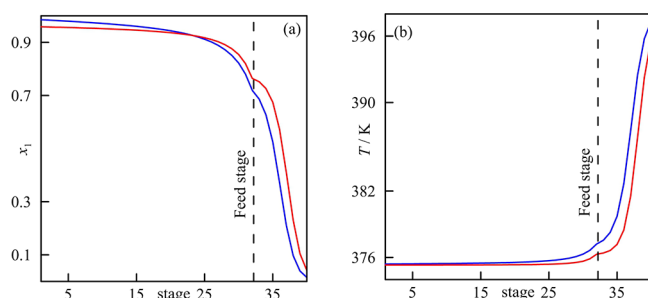
Figure 12. Profiles estimated by the AspenPlus software in the distillation operation of an equimolar binary of methyl butanoate (1) + octane (2) working at 101.32 kPa. (a) x_1 vs stage number; (b) T vs stage-number, using (red line) proposed model, eqs 19−22; (blue line) UNIFAC; (− − −) feed stage.

with the two mentioned models. The simulation with UNIFAC produces effluents in the head and bottom with compositions higher than 99% in methyl butanoate and octane, respectively, Figure 12a. Hence, the temperatures at the extremes of the tower correspond almost exactly with the boiling points $T^o_{b,i}$ of pure compounds, Figure 12b. Therefore, with the column described above it is possible to completely separate the dissolution. The location of the feed at plate 32 means that the most of the column is used to purify methyl butanoate that is obtained as a distillate. This is important since, as can be observed in Figure 5g (discontinuous line), in the region with $x_1 > 0.8$ the composition in both phases is similar (exist a pinch point), although they do not become equal (zeotropic system, as shown in Table 6). The head of the column reaches the composition $x_1 = 0.9$ at plate 26, after which the separation becomes slower: the following 25 plates serve to alter the composition from this point up to $x_1 = 0.99$. The lower region of the column requires few separation stages, due to the large distance between the compositions of both phases, see Figure 5g.

Simulation with the proposed model, eqs 2 and 3, is carried out by previously implementing said model in the commercial software and the corresponding parametrization is obtained. The result is a product at the head with a purity of 96% (v/v) in methyl butanoate, slightly lower than the result of the predictive model. Similarly, the effluent at the bottom (octane) has 4% ester content. Separation in the upper part of the column is initially faster, reaching the point $x_1 = 0.9$ at plate 27. This is because the presence of the azeotrope produces a degree of separation in the compositions, from the pinch point estimated by the UNIFAC,[57] see Figure 5g. Nonetheless, the separation stops almost completely after plate 12, where $x_1 = 0.95$, due to the proximity of the azeotropic point, $x_{1,az} = 0.974$ (Table 6). Rectification cannot, therefore, proceed beyond this point, giving rise to the lower concentration observed in Figure 12a. The faster initial separation and the subsequent stagnation results in the composition profiles of both models crossing at plate 23. According to the proposed model, separation around the lower part of the column is less effective than that estimated by UNIFAC, due to the greater quantity of ester at the feeding plate, caused by internal flows in the column. Regarding the temperature, Figure 12b, the proposed model produces a similar temperature at the head of the column, as the azeotrope is located very close to the boiling point of the pure product. However, the difference in purity at the bottoms produces an important difference in the exit temperature of this effluent, of approximately 1.6 K.

In conclusion, the simulation by Aspen-Plus[28] with UNIFAC to separate the binary methyl butanoate (1) + octane (2), shows

a complete separation of both compounds. However, the result is not real, since the system has an azeotrope that does not predict the model. Therefore, the designed equipment will not produce the devised separation, and in its operation it will stop when reaching the azeotropic composition that UNIFAC does not predict. To achieve the separation of this solution, with purity greater than 99%, it is necessary to consider other type of operations, such as extractive distillation or *pressure swing distillation*, which we have not been able to use here due to the lack of real data at low pressures.

6. CONCLUSIONS

In this work, new strategies have been employed for the thermodynamic−mathematical treatment of the experimental information of binary systems comprised of four moderate-chain alkyl alkanoates (>5) with two saturated hydrocarbons. Quality data of several properties that arise in the mixing process of the aforementioned compounds have been provided. A discussion about the behavior of solutions is presented, highlighting the nature of the different interactions, giving a satisfactory explanation for the structural model proposed, which extends to the ester + alkane group. This model satisfactorily explains the positive variation (with the increase in the hydrocarbon chain length) and negative variation (with the increase in the ester chain length) of the thermodynamic quantities arising in the mixing processes and the small gradients of these quantities with the temperature.

The presence of iso-p VLE data for the eight binaries studied generated important changes in the data presentation and treatment. A sequential methodology was established which, starting from the experimentation should conclude by using the information (verified previously) in simulation processes and to design equipment with fully guaranteed functioning. Schematically, the process consists of the succession of steps: **experimentation→verification↔modeling→simulation**, and all of them were made. A combined modeling was done of all the experimental information provided in this work using a polynomial model, which permits a multiproperty procedure to be used. In this way, a single model was generated to represent the different properties which within the working interval, adequately reflects the behavior of the solution. Parameterization was done by two procedures, one by stepwise (SSO) and another using multiobjective techniques (MOO). The MOO methodology represents the experimental data well. The repercussions of the modeling stage on verification of the VLE data is significant, and vice versa, because the **consistency test** ensures the quality of the data, guaranteeing their later use. For the first time, a methodology has been applied to the experimental information for this work to verify the quality of the iso-p VLE data, based on recommendations made in a previous work.[26] As a novelty we have incorporated the results obtained with the new method proposed by the authors,[23] adapted to the experimental information, to rigorously analyze the thermodynamic consistency, because this approach uses that model. Some deficiencies in the experimental data sets appeared in the data analysis and their effect on the global quality of set was assessed.

An estimation of the iso-p VLE data of the systems using UNIFAC was made observing that the method shows certain deficiencies to adequately represent the systems, especially in the estimation of the azeotrope of the binary methyl butanoate+octane. This system was chosen to achieve a separation of its components carrying out a simulation with AspenPlus,[28] comparing the results with those predicted by the same software using the proposed model. In summary, the deficiencies shown by UNIFAC

in the prediction of data are transferred to the simulation of the separation process, giving rise to nonreal results.

■ ASSOCIATED CONTENT

Ⓢ Supporting Information

The Supporting Information is available free of charge on the ACS Publications website at DOI: 10.1021/acs.iecr.7b04918.

Tables of properties of pure compounds (Table S1), excess volumes (Tables S2), thermal capacities of pure compounds and correlation parameters (Tables S3 and S4), excess energetic properties (Tables S5 and S6), coefficients of eq 2 for excess properties (Table S7), coefficients of eqs 19 and 26 (Table S8), NRTL equation (S9), graphical representation of excess properties (Figures S1 and S2), uncertainties of thermal capacities (Figure S3), graphic representations of results obtained in application of different consistency tests (Figure S4), results-front obtained in the modeling of one of the binary (Figure S5), and predictions of the energetic properties for all binaries by different models (Figures S6 and S7) (PDF)

■ AUTHOR INFORMATION

Corresponding Author

*E-mail: juan.ortega@ulpgc.es.

ORCID Ⓞ

Juan Ortega: 0000-0002-8304-2171

Notes

The authors declare no competing financial interest.

■ ACKNOWLEDGMENTS

■ NOMENCLATURE

A, B, C = parameters of Antoine equation
a, b, c = parameters of Antoine equation in reduced form
B_{ii} = second virial coefficient of pure compound i
B_{ij} = second virial coefficient of mixture of compounds i−j
C_{ij} = parameters of eq 3 for thermal capacity
c_j = coefficients of eq 25
c_p = molar thermal capacity, J mol^{-1} K^{-1}
c_p^E = excess molar thermal capacity, J·mol^{-1}·K^{-1}
D_A = parameter of areas test
D_w = parameter of Wisniak test
GA = genetic algorithm
g^E = excess molar Gibbs energy, J·mol^{-1}
g_i = parameters of eq 19
G_{ij} = parameters of eq 20
H_{ij} = parameters of eq 3 for enthalpy
h^E = excess molar enthalpy, J·mol^{-1}
I_i = parameter of Kojima test
k_Y = parameter of eq 3
MOO = multiobjective optimization
L_i/W_i = Parameter of Wisniak test
N = number of experimental values
n_D = refractive index
OF = objective function
p = pressure, kPa
p_i^o = vapor pressure of pure component i
q_k = Van der Waals surface parameter
R = gas constant, J·mol^{-1}K^{-1}

r_k = Van der Waals volume parameter
SSO = step-by-step optimization procedure
$s(y^E)$ = standard deviation for y^E
T = temperature, K
T_r = reduced temperature
$T_{b,i}^o$ = normal boiling point of compound i, K
VLE = vapor−liquid equilibrium
V_{ij} = parameters of eq 3 for volume
ν_i^o = molar volume of compound i, m^3·mol^{-1}
ν_i^s = saturated volume of the pure compound i, m^3·mol^{-1}
v^E = excess molar volume, m^3·mol^{-1}
x_i = molar fraction of compound i in the liquid phase
Y_{ij} = coefficients of eqs 3
y^E = generic excess property
y_i = molar fraction of compound i in the vapor phase
z_i = active fraction of the compound i, eq 3

Greek Letters

α_i = expansivity coefficients of compound i
ρ = density, kg·m^{-3}
γ_i = activity coefficient of compound i
δ = difference between two values
ϕ_i = fugacity coefficients of compound i in solution
ω = acentric factor
Φ_I = quotient between the fugacity coefficients defined in eq 9
ζ_I = parameter established in the *differential-form* of the test proposed

■ REFERENCES

(1) Fernández, L.; Perez, E.; Ortega, J.; Canosa, J.; Wisniak, J. Measurements of the excess properties and vapor-liquid equilibria at 101.32 kPa for mixtures of ethyl ethanoate+alkanes (from C$_5$ to C$_{10}$). *J. Chem. Eng. Data* **2010**, *55*, 5519−5533.

(2) Sabater, G.; Ortega, J. Excess properties and isobaric vapor−liquid equilibria for four binary systems of alkyl (methyl to butyl) methanoates with decane. *Fluid Phase Equilib.* **2010**, *291*, 18−31.

(3) Ríos, R.; Ortega, J.; Fernández, L. Measurements and correlations of the isobaric vapor- liquid equilibria of binary mixtures and excess properties for mixtures containing an alkyl (methyl, ethyl) butanoate with an alkane (heptane, nonane) at 101.3 kPa. *J. Chem. Eng. Data* **2012**, *57*, 3210−3224.

(4) Fernández, L.; Pérez, E.; Ortega, J.; Canosa, J.; Wisniak, J. Multiproperty modeling for a set of binary systems. Evaluation of a model to correlate simultaneously several mixing properties of methyl ethanoate+alkanes and new experimental data. *Fluid Phase Equilib.* **2013**, *341*, 105−123.

(5) Ríos, R.; Ortega, J.; Fernández, L.; de Nuez, I.; Wisniak, J. Improvements in the experimentation and the representation of thermodynamic properties (iso-*p* VLE and y^E) of alkyl propanoate +alkane binaries. *J. Chem. Eng. Data* **2014**, *59*, 125−142.

(6) Marrufo, B.; Rigby, B.; Pla-Franco, J.; Loras, S. Solvent effects on vapor− liquid equilibria of the binary system 1-hexene+n-hexane. *J. Chem. Eng. Data* **2012**, *57*, 3721−3729.

(7) Cripwell, J. T.; Schwarz, C. E.; Burger, A. J. Vapor−liquid equilibria measurements for the five linear C$_6$ esters with n-octane. *J. Chem. Eng. Data* **2016**, *61*, 2353−2362.

(8) Gmehling, J.; Menke, J.; Krafczyk, J.; Fischer, K. *Azeotropic Data*, 2nd ed.; VCH: Weinheim, 2004.

(9) Navarro, J.; Pintos, M.; Bravo, R.; Paz-Andrade, M. I. Excess enthalpies of (propyl ethanoate or ethyl propanoate+an n-alkane) at 298.15 K. *J. Chem. Thermodyn.* **1984**, *16*, 105−109.

(10) Lopez, M.; Paz-Andrade, M. I.; Legido, J. L.; Romaní, L.; Peleteiro, J.; Jiménez, E. Excess molar enthalpies for the (ethyl propanoate+n-hexane+n-tetradecane) system at the temperature 298.15 K. *Phys. Chem. Liq.* **1993**, *25*, 145−152.

(11) Airoldi, C.; Roca, S. Standard molar enthalpies of solvation of aliphatic esters in 1,2-dichloroethane and n-hexane. *J. Solution Chem.* **1993**, *22*, 707−713.

(12) Otín, S.; Tomás, G.; Peiró, J. M.; Gutierrez-Losa, C. Thermodynamic properties of organic oxygen compounds Excess enthalpies for some ester+hexane or + 1-bromohexane, and bromoester +hexane mixtures. *J. Chem. Thermodyn.* **1980**, *12*, 955−960.

(13) Ortega, J.; Toledo-Marante, F. Thermodynamic properties of (an ethyl ester+a branched alkane). XV. H_m^E and V_m^E values for (an ester+an alkane). *J. Chem. Thermodyn.* **2002**, *34*, 1439−1459.

(14) González, E.; Ortega, J.; Matos, J.; Tardajos, G. Thermodynamic properties of (a methyl ester+an n-alkane). II. H_m^E and V_m^E for $xCH_3(CH_2)_{u-1}CO_2CH_3$ (u = 1 to 6)+(1-x) $CH_3(CH_2)_4CH_3$. *J. Chem. Thermodyn.* **1993**, *25*, 561−568.

(15) Ortega, J.; González, E.; Matos, J.; Legido, J. Thermodynamic properties of (a methyl ester+an n-alkane). I. H_m^E and V_m^E for $xCH_3(CH_2)_{u-1}CO_2CH_3$ (u = 1 to 6)+(1-x) $CH_3(CH_2)_6CH_3$. *J. Chem. Thermodyn.* **1992**, *24*, 15−22.

(16) Jiménez, E.; Franjo, C.; Segade, L.; Legido, J. L.; Paz-Andrade, M. I. Excess molar volumes of ternary mixtures of $x_1CH_3CH_2COOCH_2CH_3+x_2CH_3(CH_2)_4CH_3+(1-x_1-x_2)$ $CH_3(CH_2)_6OH$ or $CH_3(CH_2)_7OH$ at the temperature of 298.15 K. *J. Chem. Eng. Data* **1997**, *42*, 262−265.

(17) Jiménez, E.; Franjo, C.; Menaut, C.; Segade, L.; Legido, J. L.; Paz-Andrade, M. I. Excess molar volumes of $x_1CH_3CH_2COOCH_2CH_3+x_2CH_3(CH_2)_4CH_3+(1-x_1-x_2)$ $CH_3(CH_2)_2OH$ or $CH_3(CH_2)_3OH$ at the temperature 298.15K. *J. Chem. Thermodyn.* **1997**, *29*, 117−124.

(18) Oswal, S. L.; Oswal, P.; Dave, J. P. V^E of mixtures containing alkyl acetate, or ethyl alkanoate, or ethyl bromoalkanoate with n-hexane. *Fluid Phase Equilib.* **1994**, *98*, 225−234.

(19) Matos, J.; Trenzado, J.; González, E.; Alcalde, R. Volumetric properties and viscosities of the methyl butanoate+n-heptane+n-octane ternary system and its binary constituents in the temperature range from 283.15 to 313.15 K. *Fluid Phase Equilib.* **2001**, *186*, 207−234.

(20) Arnold, D.; Greenkorn, R. A.; Chao, K.-C. Infinite-dilution activity coefficients for alkanals, alkanoates, alkanes and alkanones in n-octane. *J. Chem. Eng. Data* **1982**, *27*, 123−125.

(21) Castells, C.; Eikens, D.; Carr, P. Headspace gas chromatographic measurements of limiting activity coefficients of eleven alkanes in organic solvents at 25 °C. *J. Chem. Eng. Data* **2000**, *45*, 369−375.

(22) Ortega, J.; Espiau, F. A New Correlation Method for Vapor-Liquid Equilibria and Excess Enthalpies for Nonideal Solutions Using a Genetic Algorithm. Application to Ethanol+an n-Alkane Mixtures. *Ind. Eng. Chem. Res.* **2003**, *42*, 4978−4992.

(23) Ortega, J.; Espiau, F.; Wisniak, J. New parametric model to correlate the Gibbs excess function and other thermodynamic properties of multicomponent systems. Application to binary systems. *Ind. Eng. Chem. Res.* **2010**, *49*, 406−421.

(24) Espiau, F.; Ortega, J.; Penco, E.; Wisniak, J. Advances in the Correlation of Thermodynamic Properties of Binary Systems Applied to Methanol Mixtures with Butyl Esters. *Ind. Eng. Chem. Res.* **2010**, *49*, 9548−9558.

(25) Renon, H.; Prausnitz, J. Local composition in thermodynamic excess function for liquid mixtures. *AIChE J.* **1968**, *14*, 135−142.

(26) Wisniak, J.; Ortega, J.; Fernández, L. A fresh look at the thermodynamic consistency of vapour-liquid equilibria data. *J. Chem. Thermodyn.* **2017**, *105*, 385−395.

(27) Fernández, L.; Ortega, J.; Wisniak, J. A rigorous method to evaluate the consistency of experimental data in phase equilibria. application to VLE and VLLE. *AIChE J.* **2017**, *63*, 5125−5148.

(28) Aspen Plus of Aspentech. *Aspen Physical Properties System 2004.1. Physical Methods and Models*; Aspen Tecnhnology, Inc.: Cambridge, MA. 2004.

(29) Riddick, J. A.; Bunger, W. B.; Sakano, T. K. Organic solvents: physical properties and methods of purification. In *Techniques of Chemistry*, 4th ed.; Wiley-Interscience: New York, 1986; Vol. *II*.

(30) Ortega, J.; Matos, J. Estimation of the isobaric expansivities from several equations of molar refraction for some pure organic compounds. *Mater. Chem. Phys.* **1986**, *15*, 415−425.

(31) Zábranský, M.; Růžička, V., Jr.; Majer, V.; Domalski, E. S. Heat capacity of liquids: Volume I. Critical review and recommended values. *J. Phys. Chem. Ref. Data* **1966**, Monograph 6.

(32) TRC Thermodynamic. *Tables Non-Hydrocarbons & Hydrocarbons*; Thermodynamic Research Center, Texas A&M University System: College Station, TX, 1965 extant to 2014.

(33) Hernández, P.; Ortega, J. Vapor-liquid equilibria and densities for ethyl esters (ethanoate to butanoate) and alkan-2-ol (C3-C4) at 101.32 kPa. *J. Chem. Eng. Data* **1997**, *42*, 1090−1100.

(34) Ortega, J.; Espiau, F.; Tojo, J.; Canosa, J.; Rodriguez, A. Isobaric Vapor-Liquid Equilibria and Excess Properties for the Binary Systems of Methyl Esters+Heptane. *J. Chem. Eng. Data* **2003**, *48*, 1183−1190.

(35) Mariano, A.; Canzonieri, S.; Camacho, A.; Mainar, A.; Postigo, M. Viscometric and volumetric properties of benzene+methyl acetate, or + methyl propanoate, or + methyl butanoate binary systems at 283.15, 298.15 and 313.15 K. *Phys. Chem. Liq.* **2011**, *49*, 720−728.

(36) Mrazek, R. V.; Van Ness, H. C. Heats of mixing: Alcohol-aromatic binary systems at 25°, 35°, and 45°C. *AIChE J.* **1961**, *7*, 190−195.

(37) Ortega, J.; Peña, J.; de Alfonso, C. Isobaric vapor-liquid equilibria of ethyl acetate + etanol mixtures at 760 ± 0.5 mmHg. *J. Chem. Eng. Data* **1986**, *31*, 339−342.

(38) Sauermann, P.; Holzapfel, K.; Oprzynski, J.; Kohler, F.; Poot, W.; Loos, T. D. The ρpT properties of ethanol+hexane. *Fluid Phase Equilib.* **1995**, *112*, 249−272.

(39) Willingham, C. B.; Taylor, W. J.; Pignocco, J. M.; Rossini, F. D. Vapor pressures and boiling points of some paraffin, alkylcyclopentane, alkylcyclohexane, and alkylbenzene hydrocarbons. *J. Res. Natl. Bur. Stand.* **1945**, *35*, 219−244.

(40) Dejoz, A.; González-Alfaro, V.; Miguel, P.; Vazquez, M. I. Isobaric vapor-liquid equilibria for binary systems composed of octane, decane, and dodecane at 20 kPa. *J. Chem. Eng. Data* **1996**, *41*, 93−96.

(41) Ewing, M. B.; Sanchez Ochoa, J. C. Vapour pressures of n-hexane determined by comparative ebulliometry. *J. Chem. Thermodyn.* **2006**, *38*, 283−288.

(42) Ewing, M. B.; Ochoa, J. C. S. The vapour pressures of n-octane determined using comparative ebulliometry. *Fluid Phase Equilib.* **2003**, *210*, 277−285.

(43) Pitzer, K. S. The volumetric and thermodynamic properties of fluids. I. Theoretical basis and virial coeficients. *J. Am. Chem. Soc.* **1955**, *77*, 3427−3433.

(44) Ortega, J.; Gonzalez, C.; Peña, J.; Galván, S. Thermodynamic study on binary mixtures of propyl ethanoate and an alkan-1-ol (C_2−C_4). Isobaric vapor−liquid equilibria and excess properties. *Fluid Phase Equilib.* **2000**, *170*, 87−111.

(45) Lee, B. I.; Kesler, M. G. A generalized thermodynamic correlation based on three-parameter corresponding states. *AIChE J.* **1975**, *21*, 510−527.

(46) Bondi, A. *Physical properties of molecular liquids, cristals and glasses*; Wiley: New York. 1968.

(47) Pintos, M.; Bravo, R.; Baluja, M. C.; Paz-Andrade, M. I.; Roux-Desgranges, G.; Grolier, J.P.-E. Thermodynamics of alkanoate+alkane binary mixtures. Concentration dependence of excess heat capacities and volumes. *Can. J. Chem.* **1988**, *66*, 1179−1186.

(48) Tsonopoulos, C. Second virial coefficients of water pollutants. *AIChE J.* **1978**, *24*, 1112−1115.

(49) Smith, J. M.; Van Ness, H. C.; Abbott, M. M. *Introduction to chemical engineering thermodynamics*; McGraw-Hill: New York, 2004

(50) Redlich, O.; Kister, A. T. Thermodynamics of nonelectrolyte solutions. *Ind. Eng. Chem.* **1948**, *40*, 341−345.

(51) Fredenslund, A.; Gmehling, J.; Rasmussen, P. *Vapor-liquid equilibria using UNIFAC a group contribution method*; Elsevier: Amsterdam, 1977.

(52) Wisniak, J. A new test for the thermodynamic consistency of vapor-liquid equilibrium. *Ind. Eng. Chem. Res.* **1993**, *32*, 1531−1533.

(53) Kojima, K.; Moon, H. M.; Ochi, K. Thermodynamic consistency test of vapor-liquid equilibrium data. *Fluid Phase Equilib.* **1990**, *56*, 269–284.

(54) Van Ness, H. C. Thermodynamics in the treatment of vapor/liquid equilibrium (VLE) data. *Pure Appl. Chem.* **1995**, *67*, 859–872.

(55) Fernández, L.; Ortega, J.; Wisniak, J. New computational tool to evaluate experimental VLE and VLLE data of multicomponent systems. *Comput. Chem. Eng.* **2017**, *106*, 437–463.

(56) Ko, M.; Im, J.; Sung, J. Y.; Kim, H. Liquid-liquid equilibria for the binary system of sulfonlane with alkanes. *J. Chem. Eng. Data* **2007**, *52*, 1464–1467.

(57) Gmehling, J.; Li, J.; Schiller, M. A modified UNIFAC model. 2. Present parameter matrix and results for different thermodynamic properties. *Ind. Eng. Chem. Res.* **1993**, *32*, 178–183.